Isomeric separation and recognition of anionic and zwitterionic N-glycans from royal jelly glycoproteins

Alba Hykollari, Daniel Malzl, Barbara Eckmair, Jorick Vanbeselaere, Patrick Scheidl, Chunsheng Jin, Niclas G. Karlsson, Iain B. H. Wilson and Katharina Paschinger

Supplement

Scheme - ***Glycomic workflow employed in this study.*** Summary of the Experimental Procedures indicating serial digestion with PNGase F and PNGase Ar followed by solid-phase extraction and PA-labelling steps (for the first preparation, PNGase F and PNGase A were used in series, but without intermediate separation). Example glycans in the different pools are shown. Glycans were also released from individual SDS-PAGE separated protein bands or labelled with AEAB prior to immobilisation.

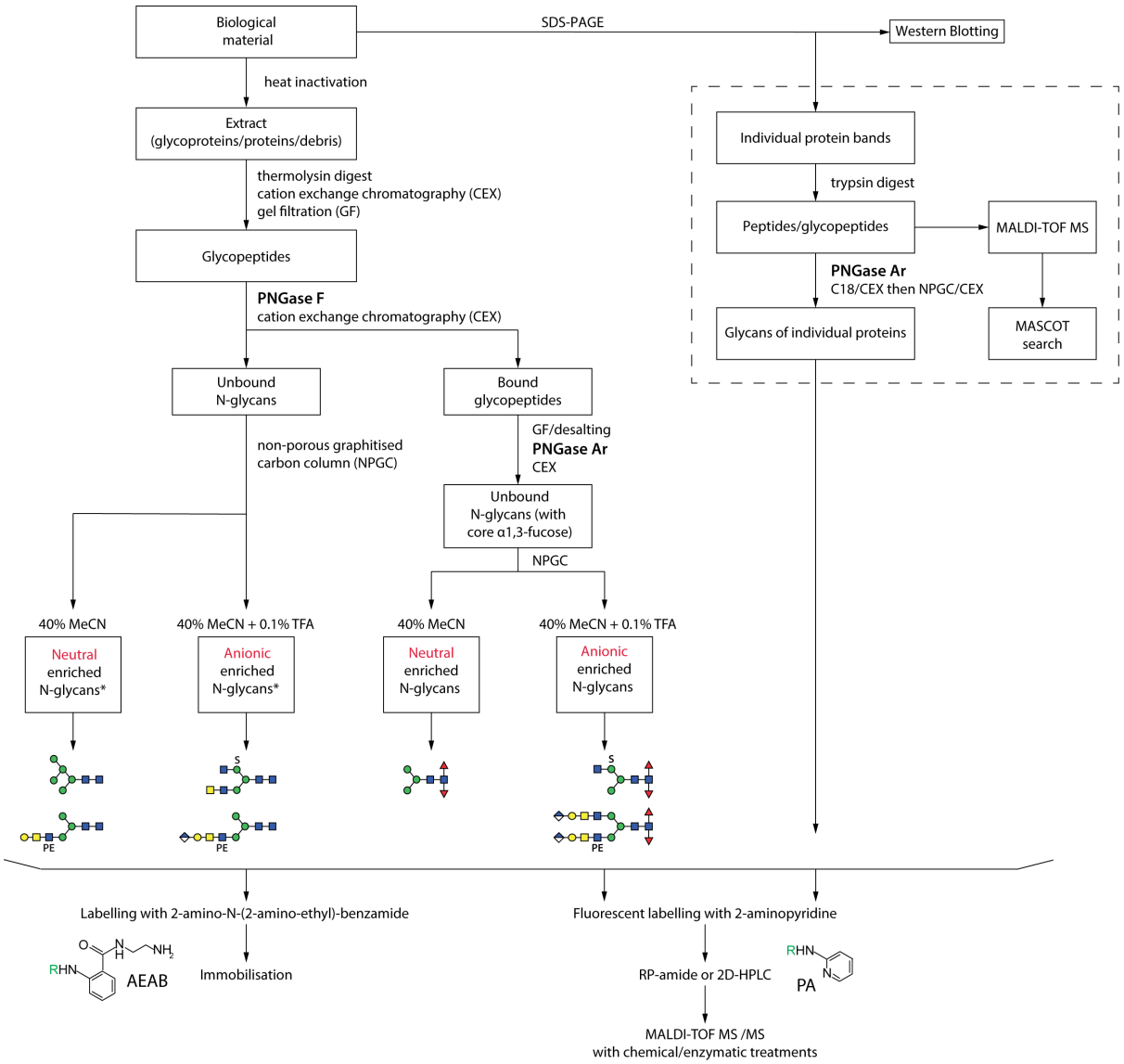

* Aliquots of the neutral and anionic PNGase F-released pools were also permethylated; for one preparation, a combined PNGase F/A-digest was performed.

Further information regarding the glycomic analyses

Definition of the level of the glycan structural analysis:

The goal was the in-depth analysis of the N-glycome of honeybee royal jelly. Thus individual glycan-containing HPLC fractions were subject to MALDI-TOF MS and MS/MS, a range of chemical and enzymatic treatments and (if appropriate) re-chromatography. Two samples were analysed: both being lots of royal jelly from the same supplier. Neutral and anionic pools were separately pyridylaminated for each sample prior to HPLC or permethylation (see *Figures 1 and 5* as well as *Supplementary Figures 1 and 2*). Additionally, single SDS-PAGE-separated protein bands were identified by tryptic peptide mapping prior to release, labelling and MS/HPLC analysis of their glycans (*Supplementary Figures 13 and 15; also Supplementary Table 2*).

Search parameters and acceptance criteria:

a. **Peak lists:** As stated in the methods section: typically 2000 shots were summed for MS and 4000 for MS/MS. Spectra were processed with the manufacturer's software (Bruker Flexanalysis 3.3.80) using the SNAP algorithm with a signal/noise threshold of 6 for MS (unsmoothed) and 3 for MS/MS (four-times smoothed).
b. **Search engine, database and fixed modifications:** All glycan data were manually interpreted and no search engine or database was employed; the fixed modification is the pyridylamine label at the reducing end ($GlcNAc_1$-PA Y-fragments of *m/z* 300).
c. **Exclusion of known contaminants and threshold:** All glycan data were manually interpreted; only peaks with an MS/MS consistent with a pyridylaminated chitobiose core were included – the 'threshold' for inclusion was an interpretable MS/MS spectrum with at least five fragment ions.
d. **Enzyme specificity:** A description of the release methods (PNGase F followed by PNGase A or Ar) is given in the methods section, whereby the latter two enzymes can cleave core α1,3-fucosylated glycans. Enzymes used during the analysis (glycosyl hydrolases) are defined in the methods by species name and supplier. Citations for in-house purified recombinant enzymes are also given. As previous experience with normalizing glycosidase amounts based on units of activity towards *p*-nitrophenyl sugars reduced digestion efficiency towards native oligosaccharides, aliquots of glycans (equivalent to 5 – 50 mV in terms of fluorescence) were incubated with 0.2 µl of the various enzyme preparations (whether commercial, desalted commercial or in-house produced) overnight at 37 °C (except for three hours in the case of insect FDL). These conditions result in no obvious unspecific removal of residues as defined by shifts in mass, MS/MS or retention times, although steric hindrance in some glycans leads to a requirement for longer incubation times (48 hours). Ammonium acetate buffers were used (supplemented with $CaCl_2$ where required) as suppliers' buffers often interfere with MALDI-TOF MS analysis; generally one-fifth of any glycosidase digest was applied directly to the target plate prior to drying and addition of matrix. Hydroflouric acid treatment (3 µl of 48% HF added to the dried glycan) was 24 or 48 hours on ice in the cold room prior to drying under vacuum; expected release of α1,3-fucose and phosphodiesters, but not of other sugars, was observed under these conditions.

   Fucosidases: Bovine kidney α-fucosidase (Sigma) does not remove core α1,3-fucose under the conditions employed, but rather core α1,6-fucose.

Glucuronidases: *E. coli* β-glucuronidase (Megazyme) removes glucuronic acid from β-linked galactose residues (e.g., as found in other insects), but apparently not from GalNAc (unpublished data); *Helix pomatia* β-glucuronidase (Sigma) removes glucuronic acid from galactose or GalNAc residues. Both glucuronidases were desalted (Vivaspin centrifugal concentration device with 10 kDa molecular weight cut-off) before use.

Hexosaminidases: Jack bean β-*N*-acetylhexosaminidase (Sigma) is a general-purpose enzyme unspecifically removing β-linked GlcNAc and GalNAc residues; *Xanthomonas manihotis* β1,2-*N*-acetylglucosaminidase (NEB, no longer sold) is a Ca^{2+}-dependent enzyme which apparently only removes unsubstituted β1,2-linked GlcNAc residues; *Streptomyces plicatus* β1,3/4-*N*-acetylhexosaminidase (NEB, 'chitinase') removes β1,4-linked GalNAc from LacdiNAc and β1,4-linked GlcNAc from chitobiose motifs; *Caenorhabditis elegans* HEX-4 is an in-house prepared recombinant enzyme which demonstrably removes β1,4-linked GalNAc residues, but in this and previous studies is not observed to remove any other HexNAc residue; insect FDL is also prepared in-house and under the described conditions only removes the β1,2-linked GlcNAc attached directly to α1,3-mannose in simple hybrid and biantennary glycans, in keeping with its proven role in the *in vivo* generation of paucimannosidic glycans.

Mannosidases: Jack bean α-mannosidase (Sigma or Prozyme) removes all α-mannose residues, but steric hindrance slows its action, e.g., digestion of core α1,6-mannose is reduced if there is a 'lower' arm modification on the core α1,3-mannose; *Xanthomonas* α1,2/3-specific mannosidases is used in this study to remove specifically the 'core' α1,3-mannose from sulphated glycans; *Helix pomatia* β-mannosidase is used to remove the β-mannose modification of core GlcNAc as previously done on marine snail glycans.

e. **Isobaric/isomeric assignments:** For isomeric species, 2D-HPLC elution and/or digestion data were used for the assignment (as described in the text).

Glycan or glycoconjugate identification

a. **Precursor charge and mass/charge (*m/z*):** All glycans detected were singly-charged. For the positive mode, the *m/z* values are for protonated forms (except for the sodiated forms of permethylated glycans), whereas in negative mode the ions are $[M-H]^-$. Depending on the glycan amount or presence of buffers in exoglycosidase preparations, the relative amounts of the H^+ and Na^+ adducts varied. Maximally two decimal places used for the *m/z*, consistent with the accuracy of MALDI-TOF MS; in the figures and due to space limitations, only one decimal place is presented. Previous data indicate an average +0.03 Da (+ 22 ppm) deviation between the measured and the calculated *m/z* values on the instrument used.

b. **All assignments:** For the glycans present in each pool, see the HIAX and RP-amide-HPLC chromatograms annotated with structures shown according to the Standard Nomenclature for Glycans. Downwardly- and upwardly-drawn core fucose and mannose residues are respectively α1,3- and α1,6-linked (see insets in *Figures 1 and 5*).

c. **Modifications observed:** Listed are the *m/z* values for glycans carrying a reducing terminal pyridylamine group as judged by presence of an *m/z* 300 $GlcNAc_1$-PA fragment. As the glycans are otherwise chemically unmodified, *Δm/z* of 123, 146, 162 and 203 correspond respectively to phosphoethanolamine, deoxyhexose (presumed to be fucose), hexose or *N*-acetylhexosamine. As glycans with *Δm/z* of 176 in this study are strongly detected in the negative mode and were glucuronidase-sensitive, this mass

difference is considered to correspond to hexuronic acid (presumed to be glucuronic acid) and not to methylhexose.

d. **Number of assigned masses:** Glycan assignments were not just based on measured mass only, but on at least MS/MS, in most cases corroborated by digest and elution data. A list of theoretical masses for all relevant compositions is presented in *Supplementary Table 1*.

e. **Spectra:** Representative annotated spectra (MS and MS/MS) defining structural elements are given in various figures. In total, annotated MS and/or MS/MS data for 70 of the approximately 100 glycans are shown on figures and are also appended in raw mzXML format (zip file). The overall data is based on some 10000 MS and MS/MS spectra.

f. **Structural assignments:** As noted in the results section, the typical oligomannosidic structures are assigned based on elution time and fragmentation pattern; the isomeric status of some structures was also confirmed by specific α1,2- and α1,2/3-mannosidase digestions, whereas the unspecific jack bean α-mannosidase fully digested $Man_{2\text{-}5}GlcNAc_2$ to $Man_1GlcNAc_2$. It is otherwise assumed that the glycans contain a trimannosyl core consistent with typical eukaryotic N-glycan biosynthesis. The presence of GlcNAcTIV (MGAT4) homologues in insects is compatible with the proposed triantennary glycans, which also have different RP-HPLC elution properties as products of GlcNAcTV (MGAT5).

   The assignments of antennal and core fucose residues are based on RP-HPLC retention time, fragmentation pattern and/or susceptibility to digestions. Core α1,3-fucose (not released with PNGase F) results in early retention on RP-HPLC, is more labile in MS/MS (equally intense Y1 $GlcNAc_1Fuc_{0\text{-}1}$-PA fragments of *m/z* 300 and 446) and is sensitive to hydrofluoric acid; core α1,6-fucose results in late retention, an intense Y1 *m/z* 446 fragment and high sensitivity to bovine α-fucosidase; antennal α1,3-fucose is sensitive to hydrofluoric acid and correlates with B-fragment ions at *m/z* 553. In general, α1,3-fucose is also associated with loss of 146 Da from the parent ion in MS/MS. Core β1,6-mannose is assigned on the basis of sensitivity to β-mannosidase (loss of *m/z* 462 Y1 fragment) as well as a comparison to LC-MS^n and RP-HPLC data on PA-glycans from a marine snail with a proven β1,3-mannose modification.

   Antennal modifications (phosphoethanolamine, glucuronic acid and *N*-acetylgalactosamine; including anomericity of some glycosidic linkages) are defined based on digestions and fragmentation patterns with rechromatography after digestion in some cases. Sulphation is detected in the negative mode and is insensitive to hydrofluoric acid, as compared to isobaric phosphate which is observed in both positive and negative modes and is sensitive to hydrofluoric acid; glycans modified with phosphoethanolamine and/or glucuronic acid are detected in both positive and negative modes and are respectively sensitive to hydrofluoric acid or glucuronidase.

   There is no evidence of any substantive in-source fragmentation of neutral terminal monosaccharides (including Lewis-type fucosylation: as evidenced by this and previous publications; see, e.g., the 2D-HPLC analysis in *Figure 2* and *Supplementary Figure 8* or the MS in various figures). The permethylation data also corroborates the assignment of the major 'native' pyridylaminated glycans and shows that the conclusions are not based on 'in source' artefacts. No N-glycan is assigned on the basis of MS alone.

   The percentage of different classes of N-glycans (oligomannosidic, glucuronylated, etc.) was estimated on the basis of HPLC and MS peak areas.

LC-MS analyses:

One selected 2D-HPLC fraction containing a core β-mannosylated N-glycan was also analyzed by online LC-MS/MS using a 10 cm × 150 µm I.D. column, prepared in-house, containing 5 µm porous graphitised carbon (PGC) particles coupled to an LTQ ion trap mass spectrometer (Thermo Scientific, Waltham, MA). Glycans were eluted using a linear gradient from 0-40% acetonitrile in 10 mM ammonium bicarbonate over 40 min at a flow rate of 10 µl/min. The eluted N-glycans were detected in negative-ion mode with an electrospray voltage of 3.5 kV, capillary voltage of -33.0 V and capillary temperature of 300 °C. Specified ions were isolated for MS^n fragmentation by collision induced dissociation (CID) with the collision energy set to 30%. Air was used as a sheath gas and mass ranges were defined dependent on the specific structure to be analysed. The data were processed using the Xcalibur software (version 2.0.7, Thermo Scientific). Glycans were identified from their MS/MS spectra by manual annotation; the nomenclature of Domon and Costello for fragment annotation was employed.

Glycoproteomic analyses:

The individual excised protein bands corresponding to the three major royal jelly proteins MRJP1, MRJP2 and MRJP3 were identified by MASCOT (Matrix Science web server, version 2.6.0) searching of the tryptic peptide fingerprints using the Swissprot database (release 2017_06, species not limited, containing 554860 entries); selected matched peptides were subject to MS/MS followed by manual annotation of the Y-ions within the Flexanalysis software in order to verify their sequence.

The sequence coverage for fingerprinting is indicated in *Supplementary Figure 13*; a list of peptides is given in *Supplementary Table 2* and raw spectra are uploaded as mzXML files. The mass tolerance was 0.3 Da (ca. 20 ppm), the potential considered modifications were carboamidomethylation of Cys residues (fixed) and oxidation of Met (variable). Trypsin generally cleaves C-terminal to Lys (K) and Arg (R); for searching purposes maximally one missed cleavage was allowed.

The glycans attached to the individual glycoproteins were analysed and assigned on the basis of MALDI-TOF MS, MS/MS and RP-HPLC data; due to the amounts, the separation into neutral and anionic pools was not performed in these experiments.

Further information regarding the glycan array analyses

1. Glycan Binding Samples	
Description of Sample	Plant lectins: biotinylated forms of concanavalin A, peanut agglutinin or wheat germ agglutinin (Vector Laboratories) Human pentraxin: Serum amyloid protein (amyloid P component from human serum, SAP; Fitzgerald) Monoclonal antibody: anti-L2/HNK-1 (clone 412; gift of Dr. Hans Bakker)
Sample modifications	(i) Alexa 647-conjugated fluorescent antibodies to detect binding of the relevant rabbit/mouse antibodies or (ii) FITC-conjugated anti-biotin to detect binding of biotinylated lectins.
Assay protocol	The slides were incubated with either: (i) biotinylated forms of plant lectins followed by incubation with anti-biotin FITC conjugate (ii) human serum amyloid P followed by incubation with anti-amyloid P IgG from rabbit and then anti-rabbit IgG AlexaFluor-647 conjugate (iii) anti-L2/HNK-1 (clone 412) followed by incubation with anti-mouse IgG AlexaFluor-647 conjugate All reagents were diluted in TTBSA and relevant wash steps were performed between their application.
2. Glycan Library	
Glycan description for defined glycans	N/A
Glycan description for undefined glycans	N-glycans were prepared by PNGase F release of glycopeptides derived by proteolysis of honeybee royal jelly and separated into neutral and anionic pools; see the experimental procedures for further details regarding isolation/labelling as well as Figure 9 and Supplementary Figure 14 for MALDI-TOF MS data. A detailed analysis of pyridylaminated royal jelly N-glycans is presented.
Glycan modifications	Glycan pools were derivatised with 2-amino-N-(2-amino-ethyl)-benzamide by reductive amination (open ring). Glycans were also either (i) pre-treated with β-galactosidase prior to printing or (ii) treated directly on the array with β-glucuronidase.
4. Arrayer (Printer)	
Description of Arrayer	Scienion Flexarrayer S1
Dispensing mechanism	Non-contact printing with the supplier's nozzles (Type 3) and a pulse of 45 µs, ca. 103 V.

Glycan deposition	Ten replicates of 0.8 nl each
Printing conditions	Derivatised glycans and oligosaccharides were mixed 1:1 with spotting buffer (300 mM sodium phosphate pH 7.5, 0.005% Tween-20); printing was at room temperature; arrays were left to hybridise overnight prior to blocking (50 mM ethanolamine in 50 mM sodium borate, pH 9.0) for 1 h at RT, washing (TBS + 0.05 % Tween-20, TBS alone, and finally H_2O) and drying.
5. Glycan Microarray	
Array layout	Fourteen subarrays per slide with ten replicates per glycan sample.
Glycan identification and quality control	Glycans on the array were pools of natural royal jelly glycans, which were checked by MALDI-TOF MS. Spotting buffer alone was used as one of the negative controls. Specificity of peanut agglutinin and anti-L2/HNK-1 was tested by respective β-galactosidase or β-glucuronidase treatments.
6. Detector and Data Processing	
Scanning hardware	Agilent G2565AA Microarray Scanner
Scanner settings	Multiple photomultiplier tube (PMT) gain values from 10-100%
Image analysis software	GenePix Pro 7
Data processing	Intensities of ten spots were taken from the GenePix software and exported into Excel without subtraction. Significance calculations and t-tests were performed in Excel.
7. Glycan Microarray Data Presentation	
Data presentation	Bar charts are shown in Figure 9 and Supplementary Figure 14.
8. Interpretation and Conclusion from Microarray Data	
Data interpretation	No software used.
Conclusions	As stated in text.

Supplementary Figure 1: MALDI-TOF MS spectra of complete neutral and anionic pools of royal jelly pyridylaminated (PA) N-glycans. Positive mode MALDI-TOF MS of the neutral pool **(A and B)** and positive **(C)** and negative **(D)** mode MALDI-TOF MS of the anionic pool of PNGase F/A-released (first preparation; A, C and D) or PNGase F-released (second preparation; B) royal jelly N-glycans after pyridylamination. Peaks (either $[M+H]^+$ or $[M-H]^-$) are annotated with abbreviated compositions (H, hexose; N, *N*-acetylhexosamine; S, sulphate; U, hexuronic acid; a.u., arbitrary units). The strong signals in the negative ion mode of the anionic-enriched pool indicate the presence of sulphated or glucuronylated N-glycans, but some residual neutral glycans are detected in the TFA-eluted fraction as are some $[M-SO_3+H]^+$ ions in the positive mode. Neither multiantennary, phosphoethanolamine-modified nor fucosylated structures were observed in the complete spectra, the off-line LC-MS approach being necessary to detect and resolve these. As shown in panels A and B, the spectra of the neutral pools of the first and second preparations were qualitatively similar, but a higher intensity of $Man_9GlcNAc_2$ was noted in the latter. The overall MALDI-TOF MS profiles of the anionic pools after PNGase F release alone or PNGase Ar after PNGase F were similar to those shown in panels C and D after combined PNGase F/A release. Raw mzXML files are included in the submitted RJ_xml.zip file.

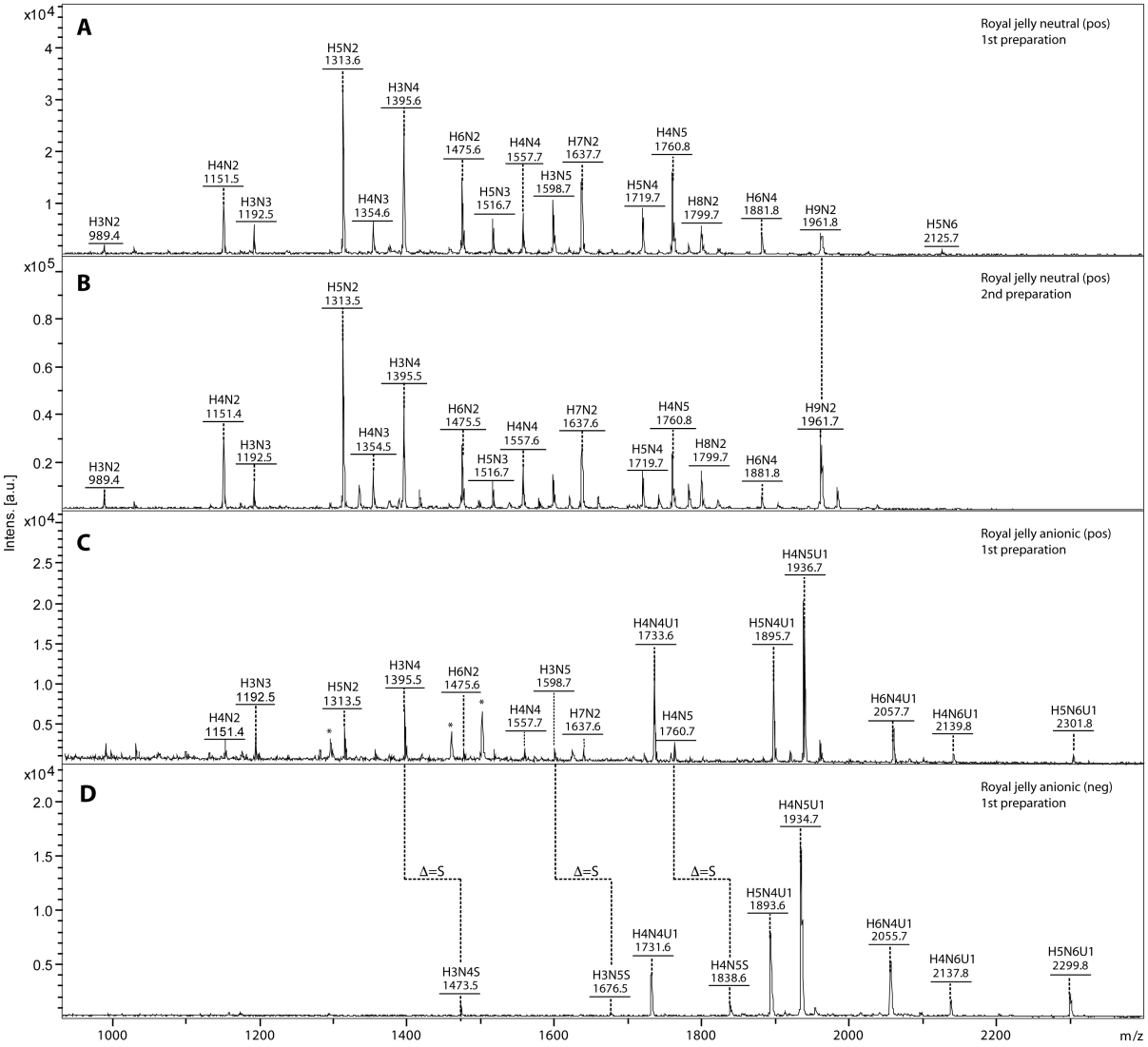

Supplementary Figure 2: MALDI-TOF MS spectra of royal jelly permethylated PNGase F-released N-glycans. (A) Positive mode MALDI-TOF MS of permethylated neutral glycans after C18 purification (50% acetonitrile elution, which is qualitatively similar to the spectrum of the 25% fraction; second preparation as in Supplementary Figure 1B). **(B and C)** Positive mode MALDI-TOF MS of permethylated anionic glycans after C18 purification (25% and 50% acetonitrile elution) to separate sulphated from glucuronylated structures; residual neutral structures from the graphitized carbon purification step preceding permethylation are present at a low level. The annotations of the sodiated ions are based on the other data in this study and selected MS/MS of permethylated hybrid and biantennary structures are shown in Supplementary Figure 3. While sulphated glycans were found in the 25% acetonitrile elution of the anionic-enriched pool (B) and glucuronylated ones in the 50% acetonitrile fraction (C), phosphoethanolamine-modified structures were not detected by this method in royal jelly (but could be in a *Penicillium* sample where one-third of the glycans possess this moiety); the underestimation of the glycome as analysed by the permethylation approach extends to triantennary structures (only one form detected) and glycans carrying either fucose or both sulphate and glucuronic acid (none detected). Raw mzXML files are included in the submitted RJ_xml.zip file.

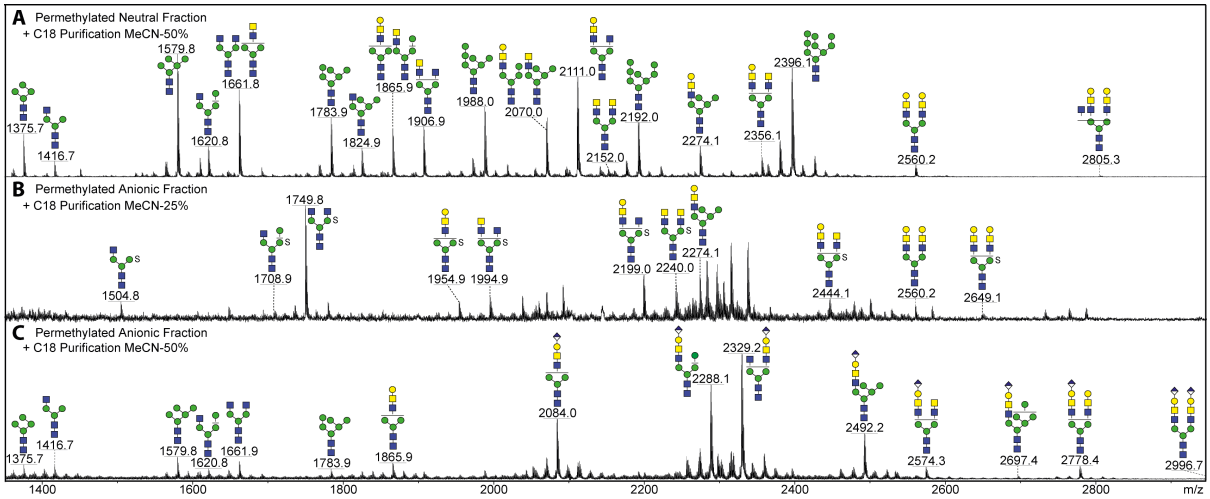

Supplementary Figure 3: MALDI-TOF MS/MS spectra of royal jelly permethylated PNGase F-released N-glycans. (A-F) Example MS/MS of permethylated sodiated glycans fragmented in positive mode (DHB as matrix); for legibility, different fragments are shown on duplicate depictions of the structures, whereas for A and B two isomers are shown (as defined by the off-line LC-MS approach; see Figure 2 in the main text for the primary analyses of $Hex_{4-5}HexNAc_4$) with discriminatory fragments at *m/z* 1157, 1361, 1402 and 1606 for A and at *m/z* 1361, 1565, 1606 and 1810 for B. The linearity of antennae (A-F) as well as the inner sulphate position (C) were clearly defined due to simple and double MS/MS fragments; galactosylated antennae are defined by the *m/z* 486 and 731 fragments and those with LacdiNAc alone by those at *m/z* 527. Furthermore, as elimination of methanol from the oxonium form of the Hex-HexNAc B2-fragment (A-E) was not detected, the data are compatible with an antennal Galβ1,3GalNAc-R linkage. As permethylation blocks all hydroxyl groups, confirmatory glycosidase digestion data are offered only by the off-line LC-MS analyses of pyridylaminated glycans. Raw mzXML files are included in the submitted RJ_xml.zip file.

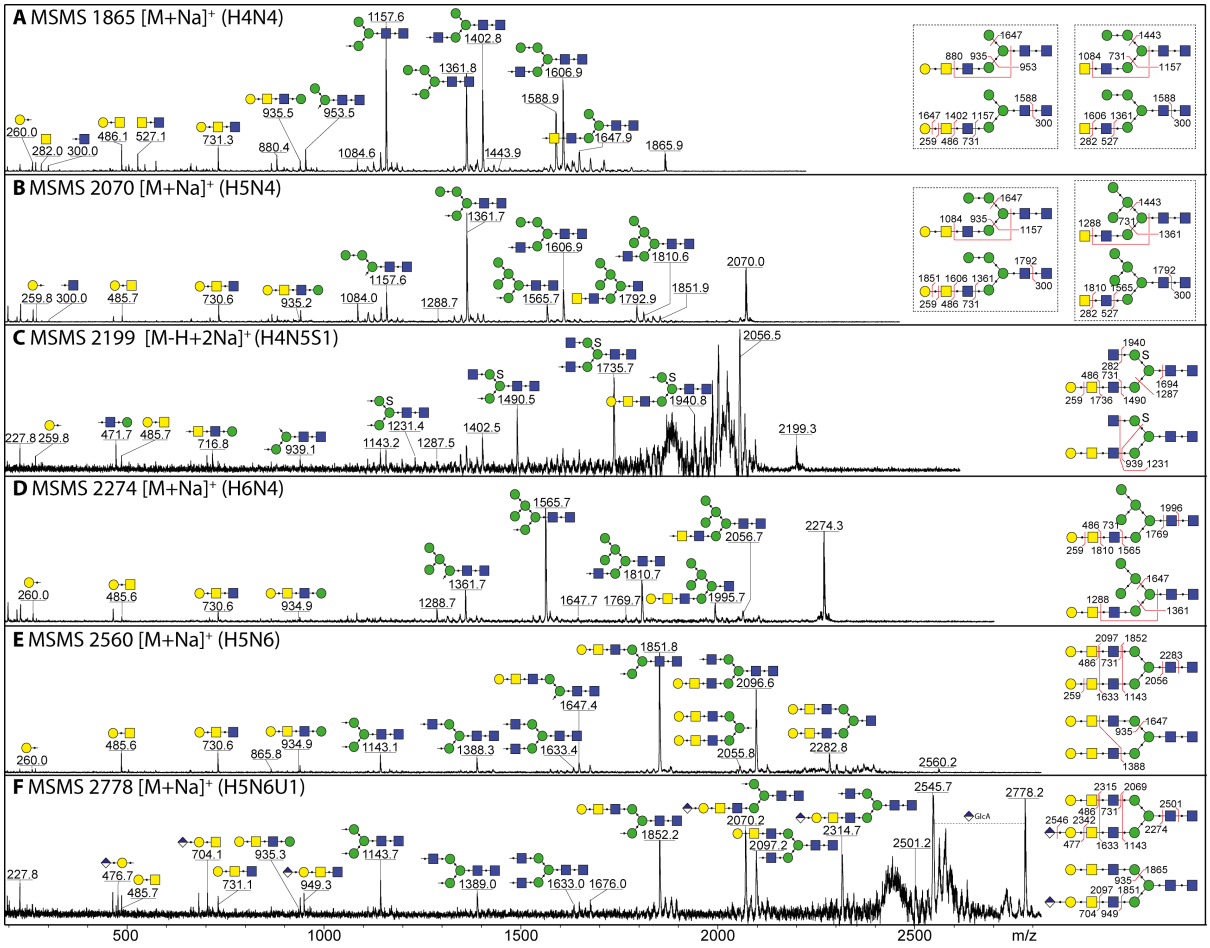

Supplementary Figure 4: Exoglycosidase digestion of major RP-HPLC fractions of neutral N-glycans. The major RP-amide fractions (7.2 and 8.2 g.u.; see Figure 1 in the main text) each containing a number of glycans were treated with both β1,3-specific galactosidase (β3Gal) and *C. elegans* β1,4-specific *N*-acetylgalactosaminidase (HEX-4) or (for the 7.2 g.u. fraction only) with jack bean α-mannosidase (JBMan) prior to MALDI-TOF MS (top panels), rechromatography (lower panels) and again analysis by MALDI-TOF-MS. Shifts in retention time and *m/z* are indicated by arrows; the different hybrid isomers in the 7.2 g.u. fraction (A_1, A_2, B_1, B_2 and B_3) were resolved by 2D-HPLC (see Figure 2 in the main text). While jack bean α-mannosidase converts $Man_{2\text{-}5}GlcNAc_2$ completely to $Man_1GlcNAc_2$ (*m/z* 665; Ia), the hybrid glycans are, due to the steric hindrance of the α1,6-mannose, only partially digested; on the other hand, combined β1,3-galactosidase/HEX-4 incubation does not affect the (pauci-)mannosidic series, but results in removal of one GalNAc from A_1 and A_2 and one Gal plus one GalNAc from B_1, B_2 and B_3 (Ib). Similarly the two biantennary glycans in the 8.2 g.u. fraction lose one GalNAc or one Gal plus one GalNAc, resulting in a single product (IIa). For further digestion and MS data on the 7.2 and 8.2 g.u. fractions, refer to Figure 2 or Suppl. Figure 5.

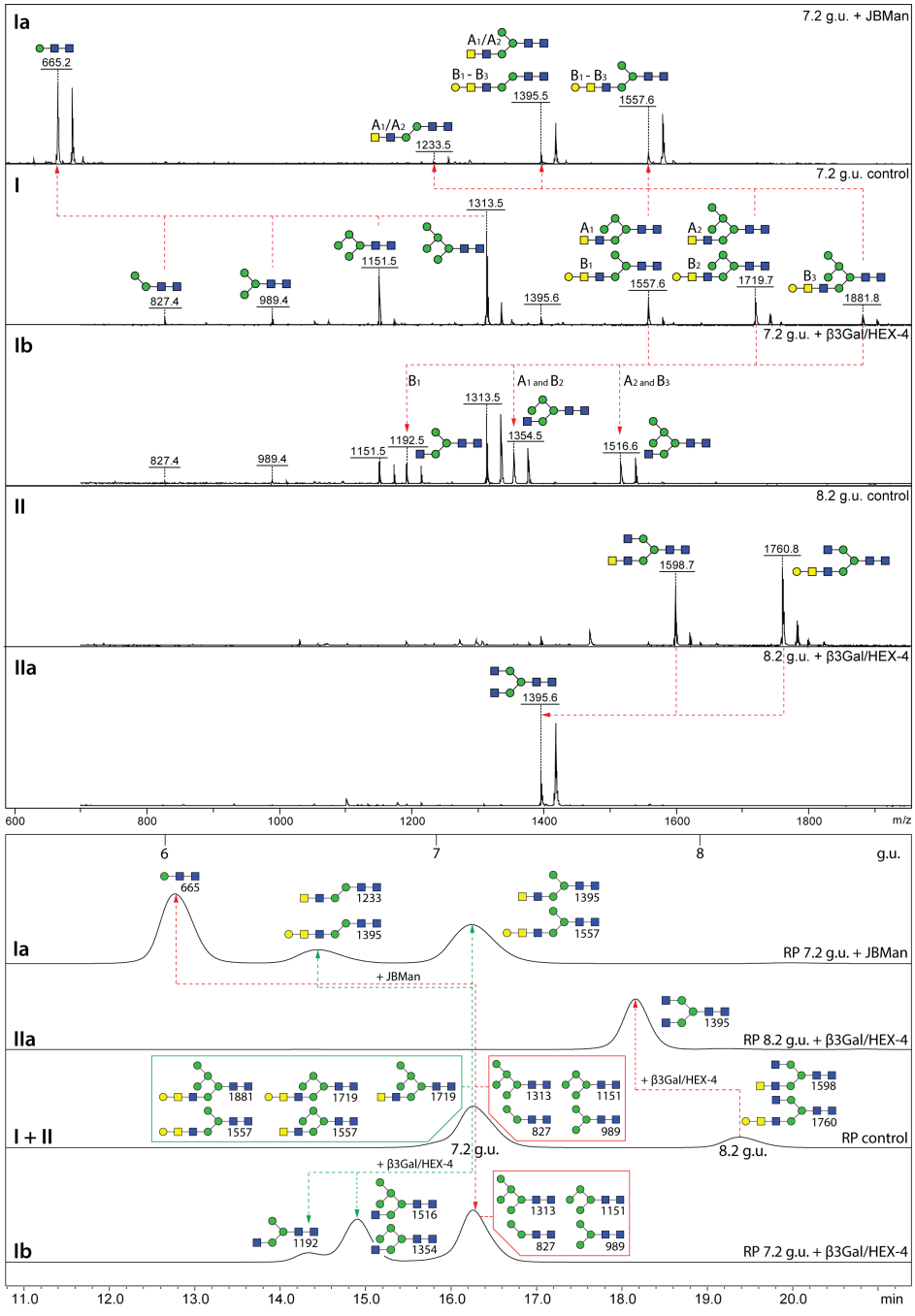

Supplementary Figure 5: Exoglycosidase digestion of isomeric biantennary neutral N-glycans. MALDI-TOF MS and MS/MS of biantennary N-glycans from the 8.2 and 9.0 g.u. fractions (A, D) with either β1,3-specific galactosidase alone (B, E) or β-*N*-acetylgalactosaminidase (HEX-4; C), sequential galactosidase/HEX-4 treatment (F) or FDL β1,2-specific *N*-acetylglucosaminidase alone (G). Thereby, the two *m/z* 1598 and two *m/z* 1760 isomers can be defined, as those eluting later are sensitive to insect FDL which is specific for the β1,2-linked GlcNAc attached to the α1,3-mannose (i.e., product of the *fused lobes* gene which removes that GlcNAc transferred by GlcNAc-transferase I). Key shifts are indicated by red or green dashed lines and diagnostic ions for the isomeric status are highlighted in turquoise or orange. Note, thereby, that the MS/MS of the *m/z* 1598 and 1760 glycans differ not so much in the occurrence of certain fragments (other than m/z 1557 in the case of a long 'lower' α1,3-arm in A), as in their intensities; isomers with longer 'upper' α1,6-arms have more distinct *m/z* 1192 fragments as compared to the *m/z* 1030 dominant for the lower arm isomers while the *m/z* 1395 digestion products (biantennary in C/F and LacdiNAc-containing in G) differ in the occurrence of *m/z* 1030 as opposed to *m/z* 407 and 989 fragment ions. Raw mzXML files corresponding to panels A, B, D and E are included in the submitted RJ_xml.zip file.

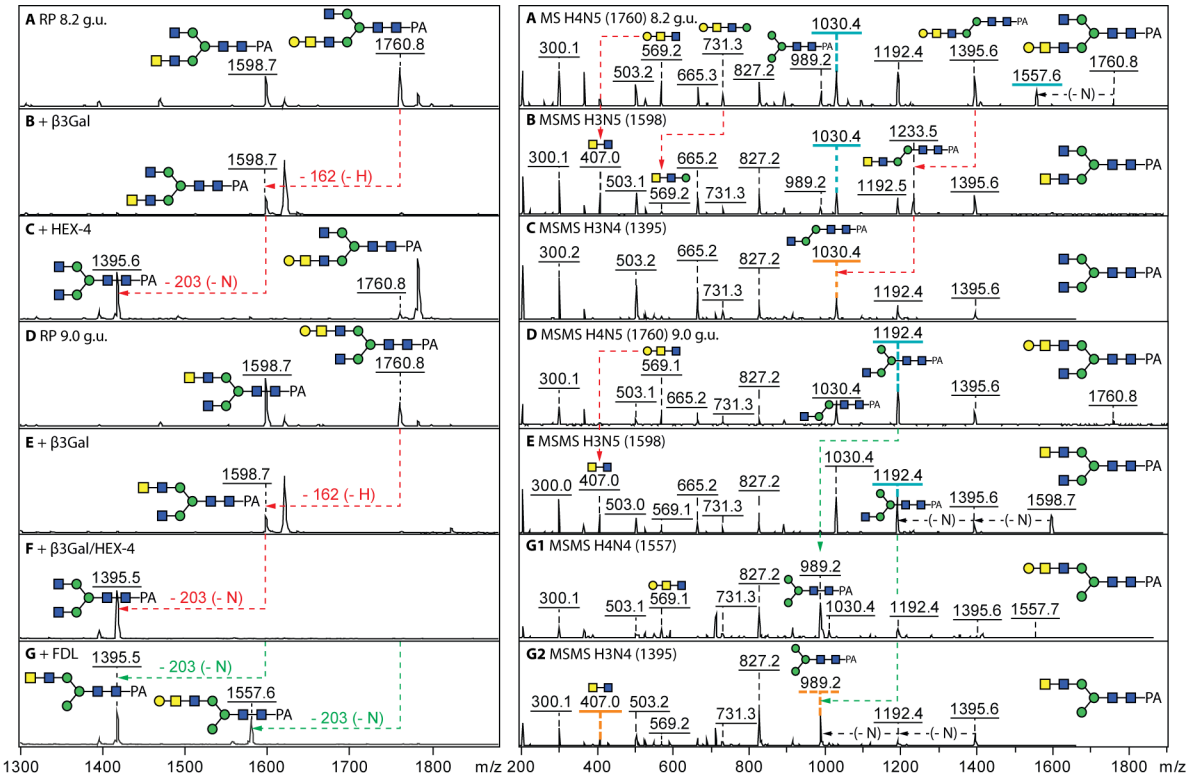

Supplementary Figure 6: Exoglycosidase digestion and MS/MS analysis of bi- and tri-antennary neutral and anionic N-glycans. (A) The triantennary N-glycans eluting at 11 g.u. (see Figure 1 in the main text) were rechromatographed after treatments with either *Xanthomonas* β1,2-*N*-acetylglucosaminidase (β2GlcNAcase), β1,3-galactosidase (β3Gal), β1,3-galactosidase in combination with HEX-4 or β1,3-galactosidase in combination with chitinase (β4HexNAcase) after prior *Xanthomonas N*-acetylglucosaminidase digestion. **(B-E)** MS/MS of the *m/z* 2329 glycan and its major triantennary digestion products. **(F-K)** MS/MS of selected neutral (F and G) and anionic (H-K) triantennary glycans annotated with significant losses or with B-/Y-fragments. Key fragments of *m/z* 1030 (B, C, E and I), 1233 (F and H), 1379 (K) and 1395 (G) are due to major fragmentation of the 'heavy' α1,3-arm modified with two antennae (indicated by a red bar); upon *Xanthomonas N*-acetylglucosaminidase treatment, the appearance of an *m/z* 827 Y-fragment allows us to conclude that a single β1,2-GlcNAc modifies the upper α1,6-arm (for example, see panel D). Raw mzXML files corresponding to panels F and G are included in the submitted RJ_xml.zip file.

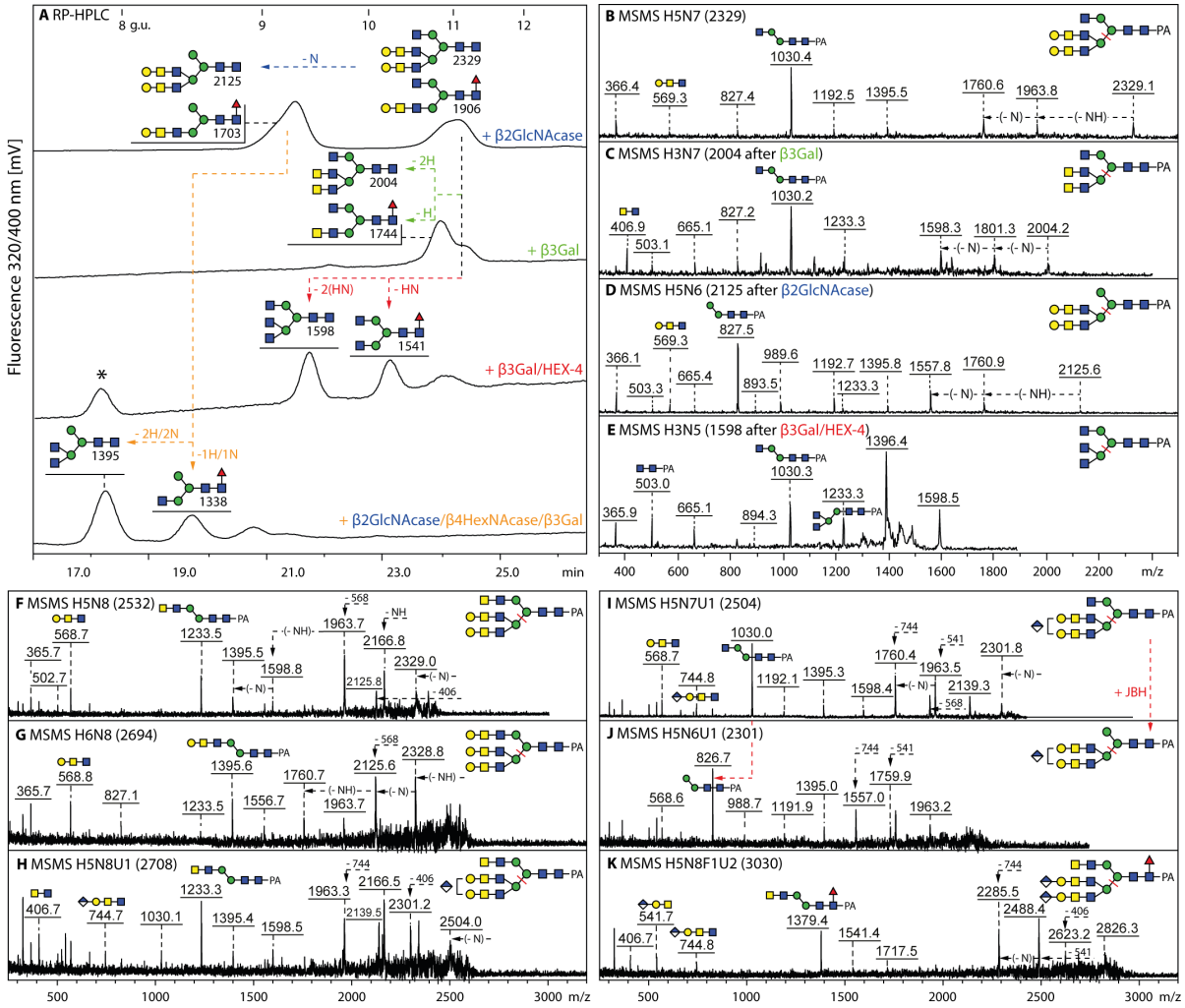

Supplementary Figure 7: Comparative analyses of β-mannosylated N-glycans. (A) Royal jelly and, as previously published, marine snail (*Volvarina*) N-glycans were fractionated on a Kinetex XB-C18 fused core RP-HPLC column; as indicated the fractions containing a core mannosylated *m/z* 1557 glycan do not co-elute. The royal jelly 6.5 g.u. fraction was re-fractionated by HIAX NP-HPLC in order to enrich the *m/z* 1557 glycan and this 2D-HPLC fraction was subject to MALDI-TOF MS (inset) and LC-MS^n (see Figure 3 in the main text), which indicated differences in fragmentation as compared to the marine snail structure. **(B)** Reinjection of the royal jelly 7.8 g.u. RP-amide and marine snail 12 g.u. Kinetex fractions onto the RP-amide column also demonstrated a lack of co-elution of the *m/z* 1557 glycans from the two species. **(C-F)** MALDI-TOF MS and MS/MS analyses of the 7.8 g.u. RP-amide fraction before and after *Xanthomonas* β1,2-*N*-acetylglucosaminidase digestion. **(G-J)** The *m/z* 1922 and 1760 glycans (2D-HPLC purified via RP-amide or Kinetex followed by HIAX) were analysed by MALDI-TOF MS/MS before and after β-mannosidase treatment resulting in loss of the *m/z* 462 fragment, thus confirming the anomericity of the core modification.

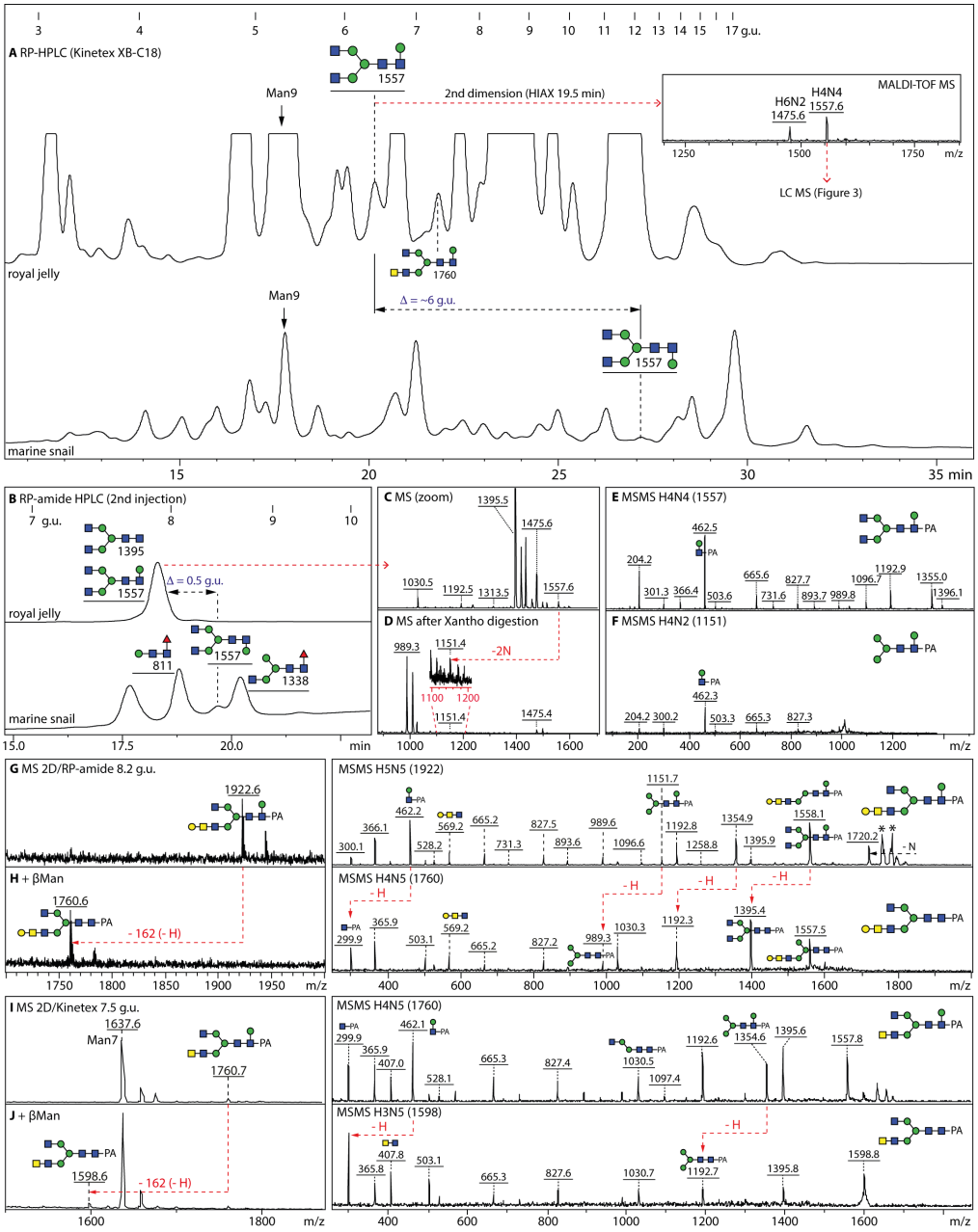

Supplementary Figure 8: MALDI-TOF MS and HPLC analysis of unmodified and phospho-ethanolamine-modified hybrid N-glycans (next page).

(I-III) Positive and negative mode MALDI-TOF MS of the 6.6 - 6.8 g.u. RP-HPLC fractions and HIAX-HPLC for 2D-separation. The doublet of *m/z* 1514/1516 in negative mode is due to $Hex_5HexNAc_3$ and $Hex_3HexNAc_4PE_1$ glycans of similar mass, which can then be resolved by HIAX fractionation; however, some hybrid structures without phosphoethanolamine are detected primarily as adducts (see asterisked ions) in the negative mode. **(A-J)** Positive mode MALDI-TOF MS of the individual 2D-separated fractions showing a similar trend of size/isomer fractionation as the parental neutral glycans (see Figure 2 of the main text). **(K-P)** Selected positive and negative mode MALDI-TOF MS/MS (see also insets) of phosphoethanolamine-modified hybrid N-glycans, including two isomers of $Hex_4HexNAc_4PE_1$ (*m/z* 1678/1680). For further data on glycans from this fraction, including MS/MS and digestion data, refer to Figure 4 in the main text as well as Supplementary Figure 9. The definition of LacdiNAc-modified glycans (e.g., isomers of *m/z* 1680) without and with galactose capping, correlating with slightly earlier elution for the former, is based on the *m/z* 528/530 and 690/692 fragments ($Hex_{0-1}HexNAc_2PE_1$; see panels L/M and N/O); the *m/z* 1313 and 1475 negative mode Y-fragments result from loss of $HexNAc_1$ or $Hex_1HexNAc_1$ from the different isomers (panels M/O), while those at *m/z* 989 and 1151 in positive mode correlate with presence of three or four mannose residues. Raw mzXML files corresponding to panels K, L, N and P are included in the submitted RJ_xml.zip file.

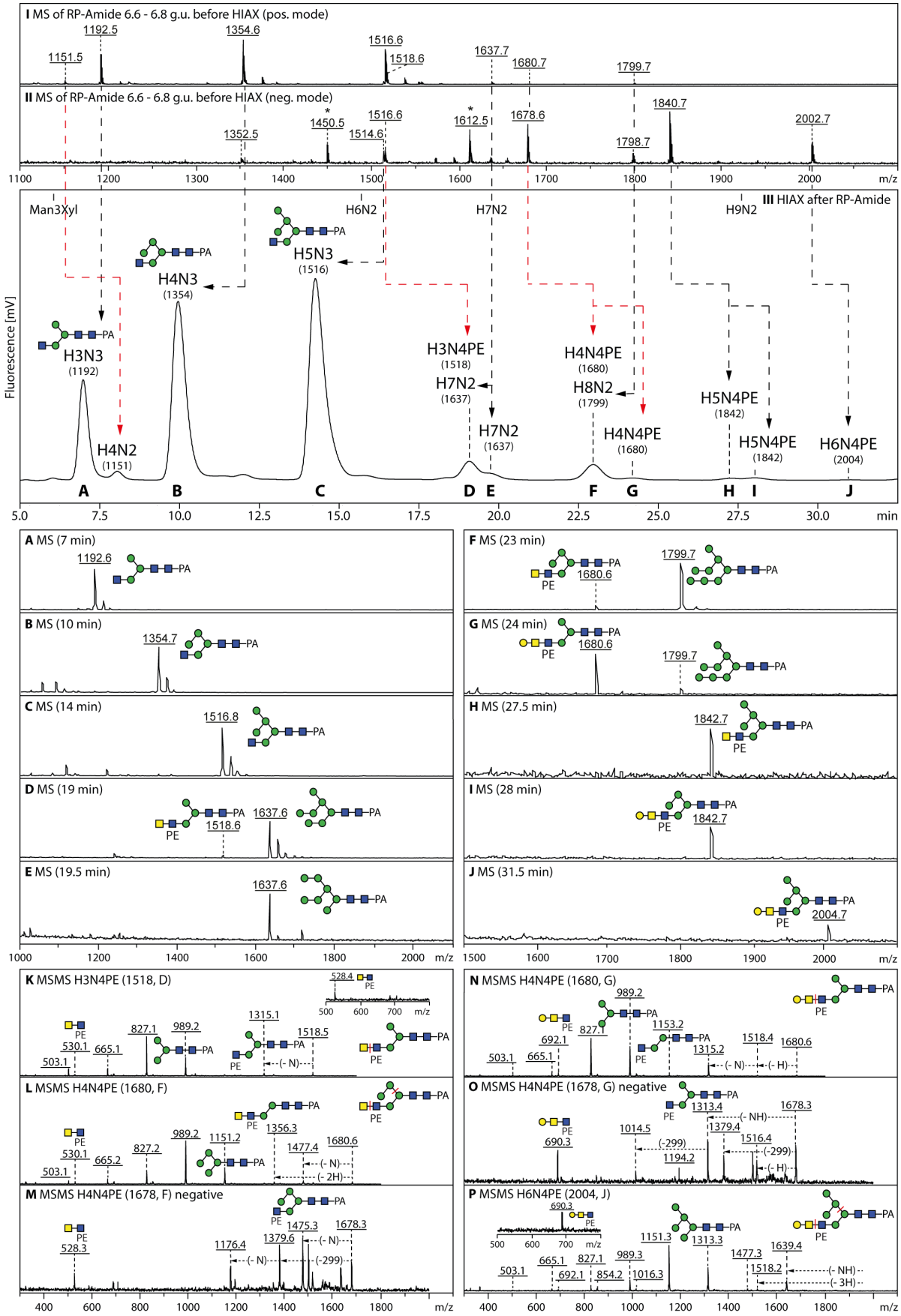
I MS of RP-Amide 6.6 - 6.8 g.u. before HIAX (pos. mode)
II MS of RP-Amide 6.6 - 6.8 g.u. before HIAX (neg. mode)
III HIAX after RP-Amide
Man3Xyl
H6N2
H7N2
H9N2
H3N3 (1192)
H4N3 (1354)
H5N3 (1516)
H4N2 (1151)
H3N4PE (1518)
H7N2 (1637)
H4N4PE (1680)
H8N2 (1799)
H5N4PE (1842)
H6N4PE (2004)
Fluorescence [mV]
m/z
min
A MS (7 min)
B MS (10 min)
C MS (14 min)
D MS (19 min)
E MS (19.5 min)
F MS (23 min)
G MS (24 min)
H MS (27.5 min)
I MS (28 min)
J MS (31.5 min)
K MSMS H3N4PE (1518, D)
L MSMS H4N4PE (1680, F)
M MSMS H4N4PE (1678, F) negative
N MSMS H4N4PE (1680, G)
O MSMS H4N4PE (1678, G) negative
P MSMS H6N4PE (2004, J)

Supplementary Figure 9: MALDI-TOF MS analysis of phosphoethanolamine-modified N-glycans. (A-H) Analysis of two 2D-HPLC separated glycans of *m/z* 1840/1842 ($Hex_5HexNAc_4PE_1$; for the HIAX chromatogram, see Supplementary Figure 8) showing negative mode spectra before and after treatments with β1,3-specific galactosidase (β3Gal), HEX-4 β-*N*-acetylgalactosaminidase and jack bean α-mannosidase (JBMan), which also aid definition of the isomeric positions for mannose or galactose; insets show a region of the negative mode MS/MS spectrum highlighting changes in the phosphoethanolamine-containing B-fragments. Refer to Figure 4 of the main text for a summarised form of these data, together with overall HPLC and MS profiles for the relevant original RP-HPLC fraction before and after hydrofluoric acid treatment. **(I-N)** Positive mode MS/MS of the above glycans and their digestion products annotated with key fragments or losses. **(O-V)** Positive mode MS/MS of selected phosphoethanolamine-modified glycans before and after hydrofluoric acid treatment highlighting the loss of the zwitterion. Raw mzXML files corresponding to panels O, Q, S and U are included in the submitted RJ_xml.zip file.

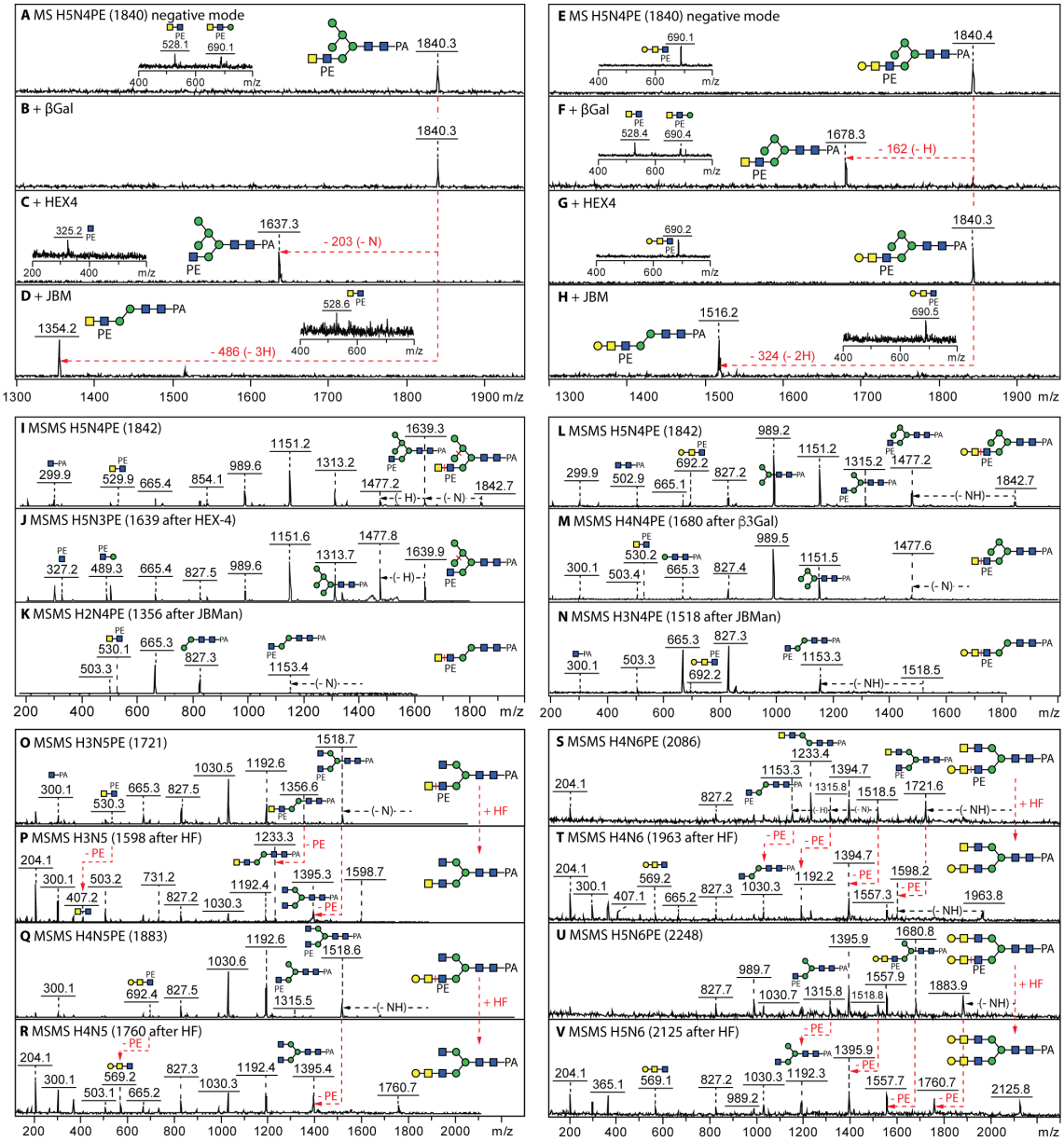

Supplementary Figure 10: HPLC and MS/MS analysis of glucuronylated glycans and their glucuronidase digestion products. RP-amide chromatograms of three *E. coli* β-glucuronidase (βGlcA) treated fractions are shown in comparison to controls (co-injection of the neutral 7.2/8.2 g.u. fractions and co-injection of aliquots of the original 6.4, 7.2 and 8.2 g.u. anionic fractions). The positive mode MALDI-TOF MS/MS **(A-L)** are alternatingly of the original and β-glucuronidase treated glycans with the changes due to loss of glucuronic acid residues being indicated with red arrows; the appearance of the *m/z* 569 $Hex_1HexNAc_2$ B-fragments after glucuronidase treatment is due to the loss of the glucuronic acid cap from the *m/z* 745 antennal B-fragments, whereas the shift to higher retention time is another indication for the removal of an anionic residue. Comparable loss of glucuronic acid from the 6.4 g.u. peak was also observed when using the *Helix pomatia* β-glucuronidase. See Figure 6 in the main text for MS and HPLC data on glycans containing both glucuronic acid and phosphoethanolamine.

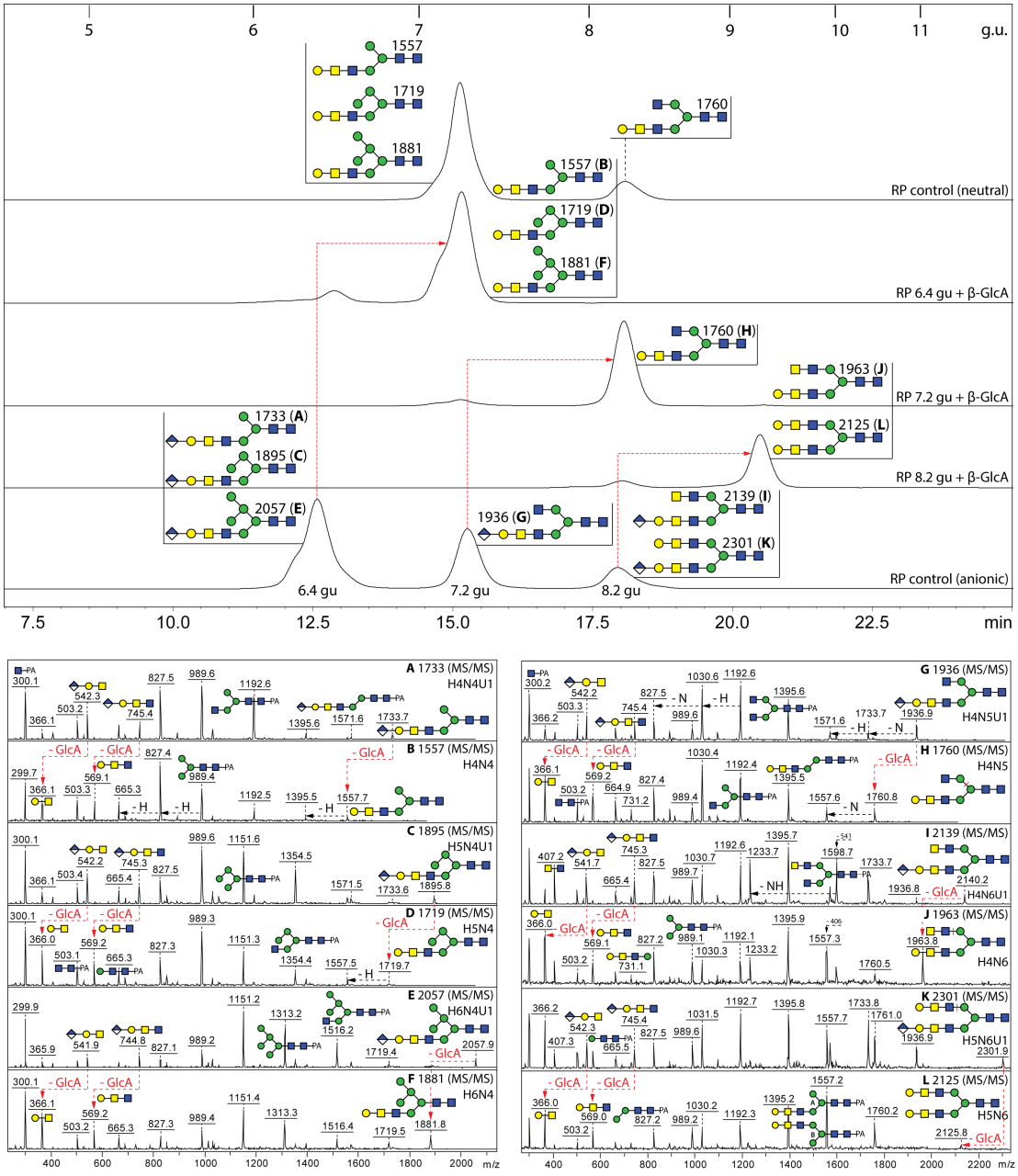

Supplementary Figure 11: Effect of hydrofluoric acid on phosphoethanolamine and α1,3-fucose modified anionic glycans. (A-D) Positive mode MALDI-TOF MS of N-glycans modified with a single phosphoethanolamine residue before and after hydrofluoric acid treatment; see Figure 6 A-G in the main text for the effect on retention time (shift from 6.0 to 6.3 g.u.) and other examples for alterations in MS/MS upon hydrofluoric acid treatment. **(E-J)** Positive mode MALDI-TOF MS of trifucosylated N-glycans modified before and after hydrofluoric acid treatment showing the spectra for the original glycan as well as the intermediate and final HF-hydrolysis products; for the effect on the retention time (shift from 4.6 to 8.0 g.u.) see Figure 8A and for the alteration in MS/MS fragmentation of the co-eluting *m/z* 2495 glycan see Figure 8B-D.

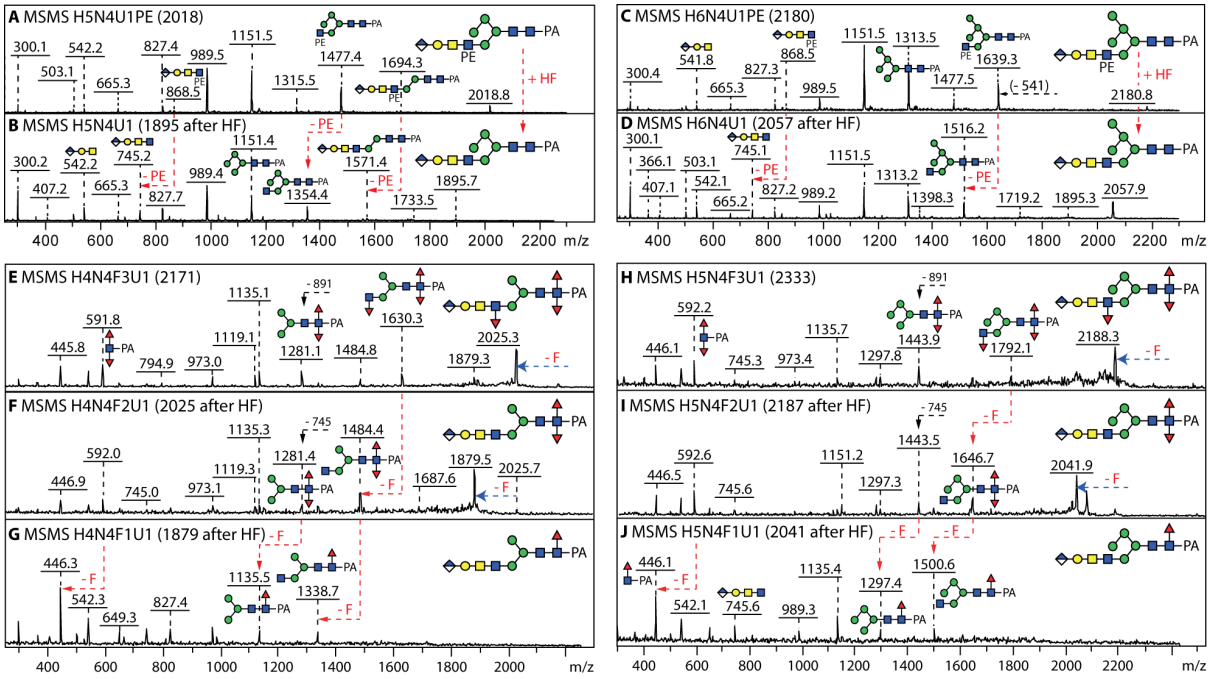

Supplementary Figure 12: MALDI-TOF MS/MS analysis of selected fucosylated and glucuronylated N-glycans. (A-J) Positive mode MALDI-TOF MS/MS of core fucosylated N-glycans in various RP-HPLC fractions of the anionic pool, including two isomers of m/z 2916 which differ in the position of a fucose residue (E and I; either antennal or core) and two phosphoethanolamine-modified glycans (B and G; *m/z* 2351 and 2408). While the *m/z* 592 Y-fragment is indicative for α1,3/α1,6-difucosylation of the core (A-E) and *m/z* 446 for the presence of a single core α1,6-fucose (F-J; the linkage being assumed on the basis of the relatively late retention times as well as bovine α-fucosidase digests not shown here; F, G and J), the *m/z* 745 and 891 B-fragments correspond to glucuronylated antennal motif lacking or possessing a 'Lewis-like' fucose residue. Both antennal and core α1,3-fucosylation result in lower retention times as compared to related structures. Core difucosylation and fucosylated LacdiNAc are elements known from, e.g., bee venom phospholipase, but these particular glucuronylated structures have not been described before in either this or in other insect species. Example effects of hydrofluoric acid on RP-HPLC and MS/MS properties of other di/trifucosylated glycans (indicative of the presence of core and antennal α1,3-fucose) are shown in Figure 8 of the main text. (**K-N**) MALDI-TOF MS and MS/MS before and after bovine α-fucosidase digestion of $Hex_4HexNAc_5Fuc_1HexA_1$; the removal of the fucose by this enzyme and the retention time (shift from 8.8 to 7.2 g.u.) are compatible with α1,6-fucosylation.

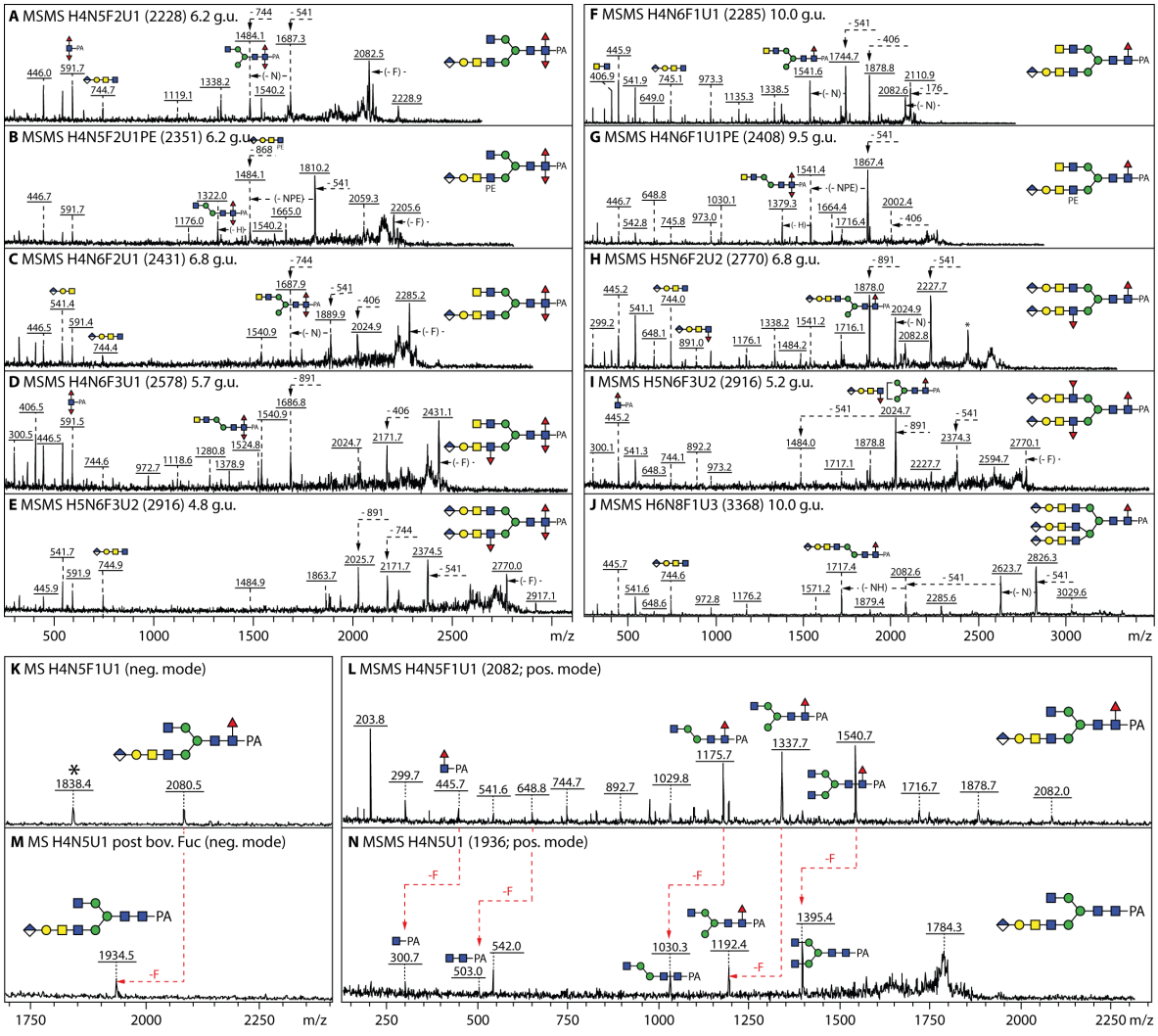

Supplementary Figure 13: Western blotting and tryptic peptide mapping of the three major royal jelly proteins (next page).

(A) Coomassie stained SDS-PAGE gel of royal jelly indicating the bands excised prior to tryptic peptide fingerprinting as well as Western blotting data: complete royal jelly was subject to SDS-PAGE followed by transfer to nitrocellulose membranes, which were then probed with either anti-horseradish peroxidase (HRP), human serum amyloid P (SAP) or human C-reactive protein (CRP) or lectins (*Aleuria aurantia* lectin, wheat germ agglutinin or peanut agglutinin). The individual bands (also seen by Ponceau S staining in red) are annotated according to the results of tryptic peptide mapping, whereby MRJP1 is the major band, MRJP2 the secondmost dominant component and MRJP3 present in three protein bands, consistent with its heterogeneity as reported in the literature; see Ref. 45 in the main text. The presence of core α1,3-fucose and phosphoethanolamine on some glycans correlates with the specificity of anti-horseradish peroxidase and human serum amyloid P (Refs. 24 and 25). As the K_d of C-reactive protein for the simple phosphoethanolamine hapten is roughly the same as that of serum amyloid P, then the binding of MRJP1 and MRJP2 by both pentraxins is explicable (note that the affinity of CRP for phosphorylcholine is higher than for phosphoethanolamine; Ref. 25). The reactivity towards *Aleuria aurantia* lectin (AAL), which recognises a range of fucosylated epitopes, wheat germ agglutinin (WGA), which binds β1,4-GalNAc, β1,4-GlcNAc and α2,3-sialic acid (the latter specificity not relevant here) and peanut agglutinin (PNA), specific for the T antigen (Galβ1,3GalNAc) is in accordance with the glycomic data (for further information on lectin specificities, see Ref. 41 and citations therein).

(B-D) The MALDI-TOF MS spectra for the three proteins (with selected peptides annotated) and the sequences (showing the coverage in red, signal peptides underlined with dashes and the predicted N-glycan sequons underlined) are shown; for a zoomed-in region of the MRJP2 spectrum containing ions corresponding to a peptide modified with different complex N-glycans refer to Figure 9C. One MRJP3 spectrum is shown which is representative for the three bands which are presumed to correspond to isoforms differing in the C-terminal repeat region; one peptide each of MRJP1 and MRJP3 was identified as being oxidised on methionine as judged by MS/MS data (indicated as 'Ox' on the MS spectra), while the *m/z* 1631 peptide in MRJP1 was verified by MS/MS, but deamidation may have occurred to yield a difference of 1 Da. Coverage is between 29 and 46%; see Supplementary Table 2 for a list of matched peptides. Minor peptides were identified from non-glycoprotein laboratory contaminants (keratin and bovine serum albumin; peptides annotated with K or B respectively), whose presence should not affect the protein-specific glycan data. The three raw mzXML files are included in the submitted RJ_xml.zip file.

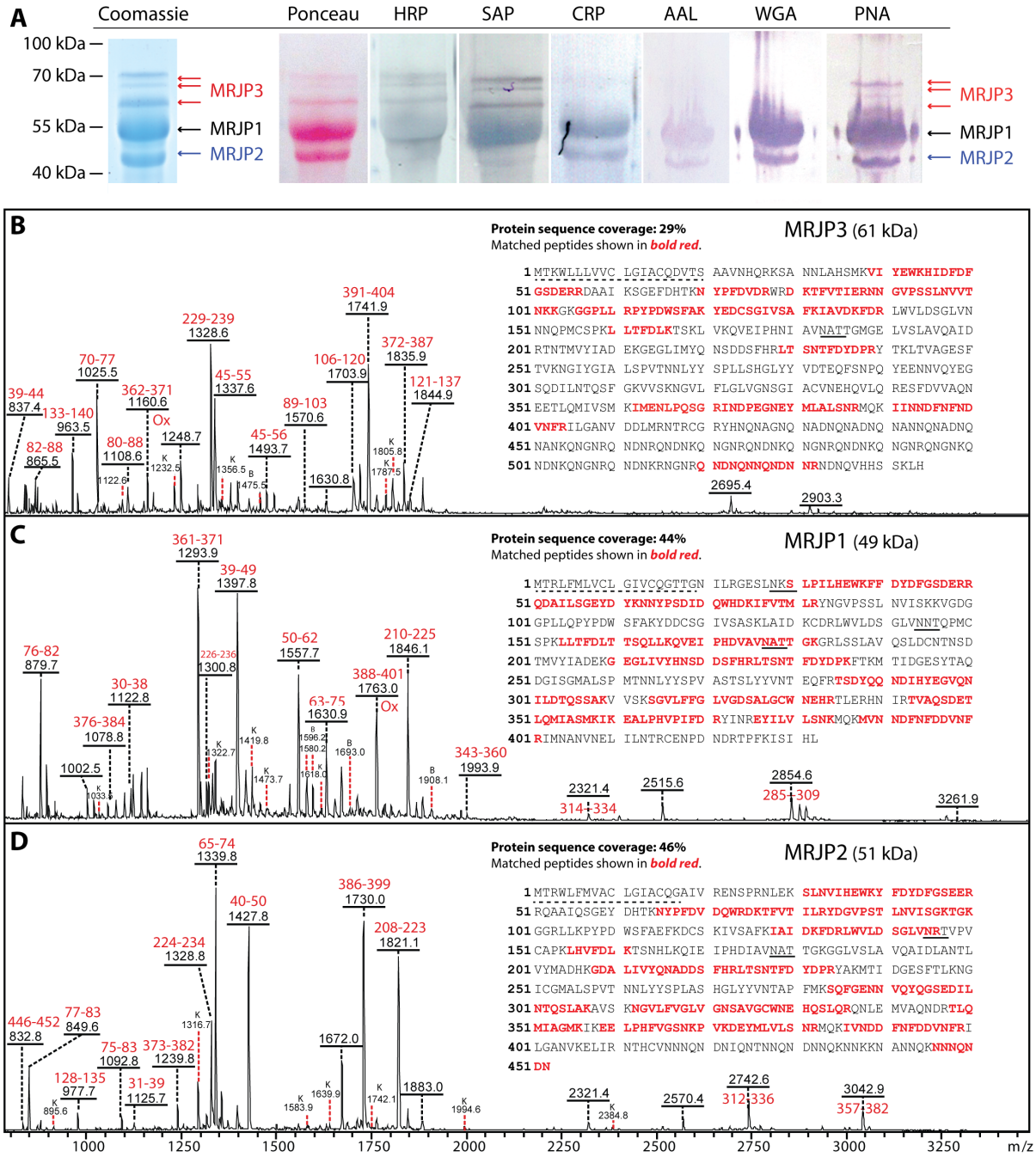
A
Coomassie
Ponceau
HRP
SAP
CRP
AAL
WGA
PNA
100 kDa
70 kDa
55 kDa
40 kDa
MRJP3
MRJP1
MRJP2
B
Protein sequence coverage: 29%
Matched peptides shown in bold red.
MRJP3 (61 kDa)
C
Protein sequence coverage: 44%
Matched peptides shown in bold red.
MRJP1 (49 kDa)
D
Protein sequence coverage: 46%
Matched peptides shown in bold red.
MRJP2 (51 kDa)
m/z

Supplementary Figure 14: Further MS and array data for AEAB-labelled royal jelly N-glycans. (A) AEAB-labelled neutral N-glycans (the protonated forms are annotated) were treated with recombinant *Aspergillus niger* β1,3/4-specific galactosidase prior to positive-mode MALDI-TOF MS (see losses of 162 Da); note that the fluorescent 2-amino-*N*-(2-amino-ethyl)-benzamide label (AEAB) confers a mass 85 Da greater than the corresponding pyridylaminated N-glycans analysed in this study. **(B)** Control and β1,3/4-galactosidase-treated AEAB-labelled neutral N-glycans or spotting buffer were printed (10 spots) and probed with either no lectin, biotinylated peanut agglutinin (PNA) or biotinylated wheat germ agglutinin (WGA) prior to application of FITC-conjugated anti-biotin; galactosidase treatment decreased the fluorescent signal for PNA, but increased it for WGA in keeping with the removal of galactose from LacdiNAc motifs. **(C)** Example positive-mode MALDI-TOF MS/MS for AEAB-labelled N-glycans showing the presence of phosphoethanolamine-modified structures in the anionic pool; for the overall MS, refer to Figure 9A of the main text. **(D)** Neutral and anionic AEAB-labelled N-glycans or spotting buffer were printed (10 spots) and probed with anti-HNK-1 either directly (with no treatment) or after on-slide native *Helix pomatia* β-glucuronidase treatment, which significantly reduced the signal for bound AlexaFluor-647-conjugated anti-mouse IgG; these data correlate with the known specificity of anti-L2/HNK-1 clone 412 (recognising an epitope on neural cell adhesion molecules and on human natural killer cells) for both sulphated and non-sulphated glucuronic acid (Ref. 44) and the presence of glucuronylated N-glycans in the anionic pool. Array data is in fluorescence units; error bars are indicated with significances of either P ≤ 0.001 (***) or P ≤ 0.01 (**).

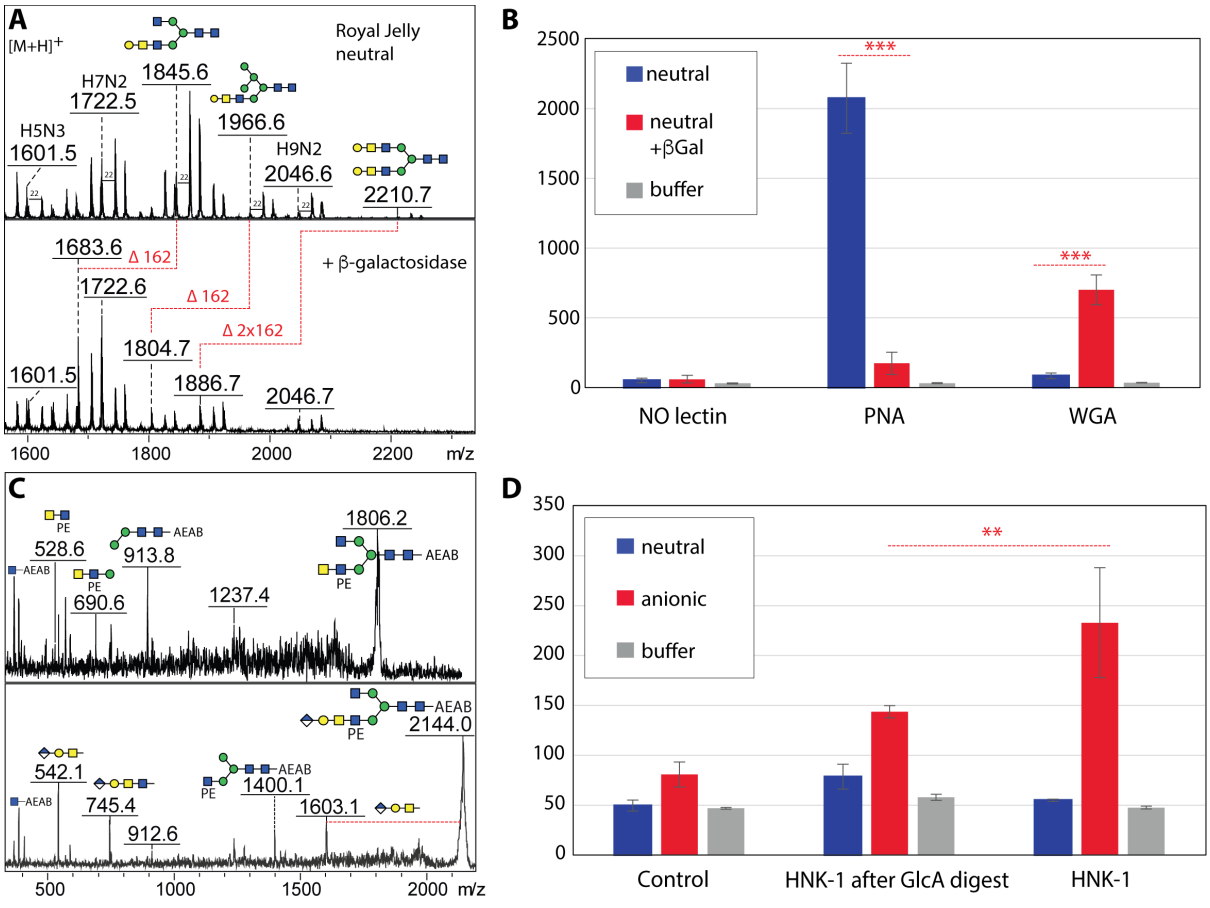

Supplementary Figure 15: Protein-specific glycoepitope analysis. RP-HPLC analysis of PNGase Ar-released N-glycans derived from individual major royal jelly proteins (MRJP1, MRJP2 and MRJP3; see also Supplementary Figure 13); the chromatograms are annotated with glycans based on MS and elution time data whereby the MRJP3 chromatogram is annotated with all identified structures and the other two with either those structures not found in the MRJP3 sample or with the *m/z* value. **(A-C)** Positive mode MALDI-TOF MS of the entire pools of released glycans with selected $[M+H]^+$ ions annotated with abbreviated compositions. **(D-G)** Example positive and negative MALDI-TOF MS spectra for two RP-HPLC fractions of MRJP1 glycans. **(H-K)** Example positive mode MALDI-TOF MS/MS of MRJP1 glycans; as the *m/z* 1881 and 1883 glycans co-fragmented, the hallmark Y-fragment doublet of *m/z* 1516/1518 resulting from the neutral loss of 365 Da is also magnified. Thus all structural elements defined in this study were present on individual glycoproteins. Raw mzXML files corresponding to panels A-C (MS) and H-K (MS/MS) are included in the submitted RJ_xml.zip file.

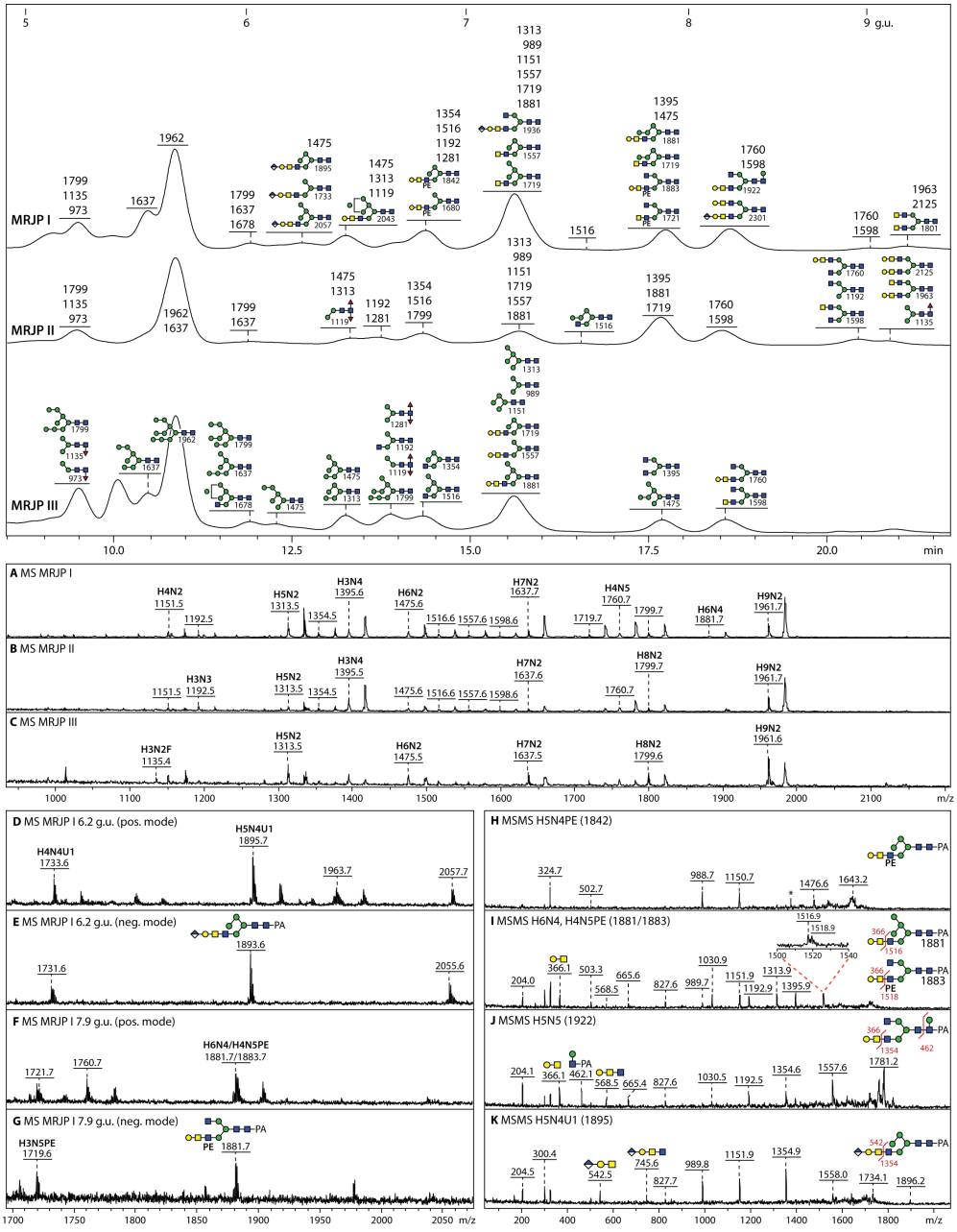

Supplementary Table 1: Theoretical *m/z* values of relevant glycan compositions are listed as $[M+H]^+$ and, for structures modified with phosphoethanolamine, sulphate and/or glucuronic acid, as $[M-H]^-$ (one decimal place); *m/z* values given in italics are those for in-source loss in positive mode of sulphate from sulphated glycans (i.e., $[M-SO_3+H]^+$ ions). H, hexose (mannose or galactose), N, *N*-acetylhexosamine (GalNAc or GlcNAc); F, deoxyhexose (fucose); U, hexuronic acid (glucuronic acid); S, sulphate; PE, phosphoethanolamine. For observed *m/z* values refer to the relevant figures which include annotated MS and MS/MS spectra.

composition	$[M+H]^+$	$[M-H]^-$
H2N2	827.3	
H2N2F	973.4	
H3N2	989.4	
H2N2F1S	*(973.4)*	1051.4
H3N2F1	1135.5	
H4N2	1151.4	
H3N3	1192.5	
H3N2F1S	*(1135.5)*	1213.4
H3N3S	*(1192.5)*	1270.4
H5N2	1313.5	
H3N3F1	1338.5	
H4N3	1354.5	
H3N2F2S	*(1281.5)*	1359.5
H3N4	1395.6	
H3N4S	*(1395.6)*	1473.5
H6N2	1475.6	
H5N3	1516.6	
H3N4PE	1518.6	1516.6
H3N4F1	1541.6	
H4N4	1557.6	
H3N3F2S	*(1484.6)*	1562.5
H3N4U1	1571.6	1569.6
H3N5	1598.6	
H3N4F1S	*(1541.6)*	1619.6
H4N4S	*(1557.6)*	1635.5
H7N2	1637.6	
H3N5S	*(1598.6)*	1676.5
H6N3	1678.6	
H4N4PE	1680.6	1678.6
H5N4	1719.7	
H3N5PE	1721.6	1719.6
H4N4U1	1733.6	1731.6
H3N5F1	1744.7	
H4N5	1760.7	
H8N2	1799.7	
H3N6	1801.7	
H4N5S	*(1760.7)*	1838.6
H5N4PE	1842.7	1840.7
H4N4U1PE	1856.6	1854.6
H4N4F1U1	1879.7	1877.7
H3N6S	*(1801.7)*	1879.7
H6N4	1881.7	
H4N5PE	1883.7	1881.7
H5N4U1	1895.7	1893.7
H4N5F1	1906.7	
H5N5	1922.7	
H3N6PE	1924.7	1922.7
H4N5U1	1936.7	1934.7
H3N6F1	1947.8	
H9N2	1961.7	
H4N6	1963.8	
H6N4PE	2004.7	2002.7
H3N7	2004.8	
H5N4U1PE	2018.7	2016.7
H4N4F2U1	2025.8	2023.7
H5N4F1U1	2041.7	2039.7
H4N6S	*(1963.8)*	2041.7
H7N4	2043.8	
H6N4U1	2057.7	2055.7
H4N5U1PE	2059.7	2057.7
H4N5F1U1	2082.8	2080.8
H4N6PE	2086.8	2084.8
H5N5U1	2098.8	2096.8
H4N6F1	2109.8	
H5N6	2125.8	
H4N6U1	2139.8	2137.8
H4N7	2166.8	
H4N4F3U1	2171.8	2169.8
H6N4U1PE	2180.8	2178.8
H5N4F2U1	2187.8	2185.8
H4N5F1U1PE	2205.8	2203.8
H7N4U1	2219.8	2217.8
H4N5F2U1	2228.8	2226.8
H5N6PE	2248.8	2246.8
H4N6U1PE	2262.8	2260.8
H4N6F1U1	2285.9	2283.8
H5N6U1	2301.8	2299.8
H5N7	2328.9	
H5N4F3U1	2333.9	2331.8
H4N7U1	2342.9	2340.9
H6N4F2U1	2349.9	2347.8
H4N5F2U1PE	2351.8	2349.8
H4N5F3U1	2374.9	2372.9
H4N6F1U1PE	2408.9	2406.8
H5N6U1PE	2424.9	2422.8
H4N6F2U1	2431.9	2429.9
H5N6F1U1	2447.9	2445.9
H5N6U2	2477.9	2475.9
H6N4F3U1	2495.9	2493.9
H5N7U1	2504.9	2502.9
H5N8	2531.9	
H5N6F1U1PE	2570.9	2568.9
H4N6F3U1	2578.0	2576.0
H5N6F2U1	2594.0	2591.9
H5N6F1U2	2623.9	2621.9
H5N6F1U2S	*(2623.9)*	2701.9
H6N8	2694.0	
H5N8U1	2708.0	2706.0
H5N6F3U1	2740.0	2738.0
H5N6F1U2PE	2746.9	2744.9
H5N6F2U2	2770.0	2768.0
H5N7F1U2	2827.0	2825.0
H5N6F2U2S	*(2770.0)*	2847.9
H6N8U1	2870.1	2868.0
H5N6F2U2PE	2893.0	2891.0
H5N6F3U2	2916.1	2914.0
H5N6F3U2S	*(2916.1)*	2994.0
H5N8F1U2	3030.1	3028.1
H6N8F1U2	3192.2	3190.1
H6N8F1U3	3368.2	3366.2
H6N8F1U3S	*(3368.2)*	3446.1

Supplementary Table 2: Theoretical and observed *m/z* values (all $[M+H]^+$) for the tryptic peptide mapping of major royal jelly glycoproteins are given together with the sequence of the peptides, mass deviations (ΔM) and numbers of missed cleavages (MC); for the peptide mass spectra refer to Supplementary Figure 13 as well as the corresponding raw mzXML MS files. The search parameters were for trypsin (cuts C-term side of KR unless next residue is P) with carboxyamidylation as a fixed modification, oxidation as a variable modification and windows of 0.3 Da; the Swissprot database available in July 2017 was searched using Mascot. For the glycoform variants of the MRJP2 peptide 136-146, refer to Figure 9C; the experimental and calculated masses for deglycosylated peptides (Δ = 1 Da) were not included in the score calculation, but are compatible with the deamidation of Asn to Asp.

MRJP1 (*Apis mellifera*; MRJP1_APIME, Score: 106)

Start–End	Observed	Mr(expt)	Mr(calc)	ΔM	MC	Peptide
30 – 38	1122.6450	1121.6377	1121.6233	0.0144	0	K. SLPILHEWK.F
39 – 49	1397.5710	1396.5637	1396.5572	0.0065	0	K. FFDYDFGSDER.R
50 – 62	1557.7640	1556.7567	1556.7471	0.0097	1	R. RQDAILSGEYDYK.N
76 – 82	879.5130	878.5057	878.5048	0.0009	0	K. IFVTMLR.Y
154 – 166	1492.8190	1491.8117	1491.8548	-0.0431	0	K. LLTFDLTTSQLLK.Q
167 – 182	1679.8090	1678.8017	1677.8686	0.9331	0	K. QVEIPHDVAVNATTGK.G (deglyco)
210 – 225	1845.8500	1844.8427	1844.8442	-0.0015	0	K. GEGLIVYHNSDDSFHR.L
226 – 236	1300.6140	1299.6067	1299.5983	0.0084	0	R. LTSNTFDYDPK.F
285 – 309	2854.3300	2853.3227	2853.3053	0.0174	0	R. TSDYQQNDIHYEGVQNILDTQSSAK.V
314 – 334	2321.1240	2320.1167	2320.1059	0.0108	0	K. SGVLFFGLVGDSALGCWNEHR.T
343 – 360	1993.9780	1992.9707	1993.0224	-0.0516	1	R. TVAQSDETLQMIASMKIK.E
361 – 371	1293.6910	1292.6837	1292.6877	-0.0040	0	K. EALPHVPIFDR.Y
376 – 384	1078.6120	1077.6047	1077.6070	-0.0023	0	R. EYILVLSNK.M
388 – 401	1762.7570	1761.7497	1761.7417	-0.0080	0	K. MVNNDFNFDDVNFR.I (Met-Ox)

MRJP2 (*Apis mellifera*; MRJP2_APIME, Score: 131)

Start–End	Observed	Mr(expt)	Mr(calc)	ΔM	MC	Peptide
31 – 39	1125.7480	1124.7407	1124.5978	0.1429	0	K. SLNVIHEWK.Y
40 – 50	1427.6080	1426.6007	1426.5677	0.0330	0	K. YFDYDFGSEER.R
65 – 74	1339.6180	1338.6107	1338.5993	0.0114	0	K. NYPFDVDQWR.D
75 – 83	1092.7850	1091.7777	1091.6339	0.1438	1	R. DKTFVTILR.Y
77 – 83	849.6110	848.6037	848.5120	0.0917	0	K. TFVTILR.Y
84 – 100	1735.8970	1734.8897	1734.9152	-0.0255	1	R. YDGVPSTLNVISGKTGK.G
128 – 135	977.6270	976.6197	976.5342	0.0856	1	K. IAIDKFDR.L
136 – 146	1272.6580	1271.6507	1270.7034	0.9473	0	R. LWVLDSGLVNR.T (deglyco)
155 – 161	871.6330	870.6257	870.4963	0.1294	0	K. LHVFDLK.T
208 – 223	1821.0830	1820.0757	1819.8489	0.2268	0	K. GDALIVYQNADDSFHR.L
224 – 234	1328.7680	1327.7607	1327.6044	0.1563	0	R. LTSNTFDYDPR.Y
284 – 307	2670.4600	2669.4527	2669.2569	0.1958	0	K. SQFGENNVQYQGSEDILNTQSLAK.A
312 – 336	2741.3340	2740.3267	2740.3504	-0.0237	0	K. NGVLFVGLVGNSAVGCWNEHQSLQR.Q
348 – 356	992.5900	991.5827	991.5194	0.0633	0	R. TLQMIAGMK.I
359 – 372	1580.8170	1579.8097	1579.8358	-0.0261	0	K. EELPHFVGSNKPVK.D
373 – 382	1239.7690	1238.7617	1238.5965	0.1652	0	K. DEYMLVLSNR.M
386 – 399	1729.7860	1728.7787	1728.7744	0.0043	0	K. IVNDDFNFDDVNFR.I
446 – 452	832.5800	831.5727	831.3107	0.2620	0	K. NNNQNDN.-

MRJP3 (*Apis mellifera*; MRJP3_APIME, Score: 70)

Start–End	Observed	Mr(expt)	Mr(calc)	ΔM	MC	Peptide
39 – 44	837.4600	836.4527	836.4432	0.0095	0	K. VIYEWK.H
45 – 55	1337.6300	1336.6227	1336.5684	0.0543	0	K. HIDFDFGSDER.R
45 – 56	1493.7400	1492.7327	1492.6695	0.0632	1	K. HIDFDFGSDERR.D
70 – 77	1025.4970	1024.4897	1024.4614	0.0283	0	K. NYPFDVDR.W
80 – 88	1108.6280	1107.6207	1107.5924	0.0283	1	R. DKTFVTIER.N
82 – 88	865.4960	864.4887	864.4705	0.0182	0	K. TFVTIER.N
89 – 103	1570.6680	1569.6607	1569.8475	-0.1867	1	R. NNGVPSSLNVVTNKK.G
106 – 120	1703.9440	1702.9367	1702.8831	0.0536	0	K. GGPLLRPYPDWSFAK.Y
121 – 137	1844.9330	1843.9257	1843.9026	0.0231	1	K. YEDCSGIVSAFKIAVDK.F
133 – 140	963.5500	962.5427	962.5185	0.0242	1	K. IAVDKFDR.L
160 – 166	849.5280	848.5207	848.5007	0.0200	0	K. LLTFDLK.T
229 – 239	1328.6580	1327.6507	1327.6044	0.0463	0	R. LTSNTFDYDPR.Y
362 – 371	1160.6000	1159.5927	1159.5655	0.0272	0	K. IMENLPQSGR.I (Met-Ox)
372 – 387	1835.9000	1834.9027	1834.8519	-0.0452	0	R. INDPEGNEYMLALSNR.M
391 – 404	1741.8930	1740.8857	1740.8220	0.0637	0	K. IINNDFNFNDVNFR.I
520 – 532	1587.7010	1586.6937	1586.6418	0.0520	0	R. QNDNQNNQNDNNR.N